Report on 2020
Conesus Lake Monitoring Program:
In-Lake Studies

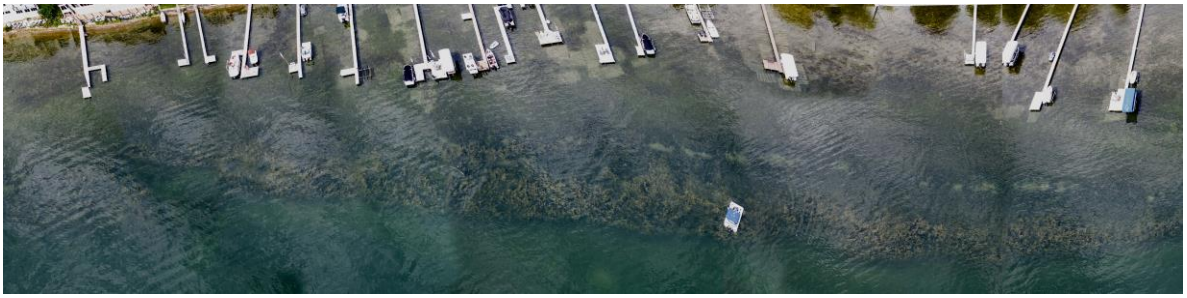

I. Current and Historical Patterns (2000-2020) of Macrophyte Biomass and Standing Crop in Eurasian Watermilfoil-Dominated Beds

by
*Isidro Bosch, ^Michael Chislock, [+]Karl Hanafin, *Erin Kane,
^Jennifer Beideck, *Amanda Crowe, *Anna DeHart and *Ethan Warick

II. Tributary Plume Dispersion Patterns: Observations from Aerial Surveillance and *In Lake* Conductivity Sensors

by
[+]Karl Hanafin, Isidro Bosch and Michael Chislock

III. Description of Late-Season Phytoplankton Bloom Related to Water Column Mixing Events

by
*Brooke Drexler, *Katheryne Hibbert-Nelson, *Sarah Metz
and Isidro Bosch

*State University of New York at Geneseo
^State University of New York at Brockport
[+]Livonia, NY

Report Submitted to
The Livingston County Planning Department
January 15, 2021

Table of Contents

List of Tables

List of Figures

I. Summary

- The last comprehensive study of the Conesus Lake macrophytes was completed in 2012. During the summer 2020, we studied the macrophyte community primarily to determine if the invasive Eurasian watermilfoil (*Myriophyllum spicatum*) continued to form large, dense macrophyte beds in different parts of the lake.

- A lake-wide survey of macrophytes and filamentous algal cover was conducted on July 27. Milfoil-dominated beds continue to be prominent is some areas of the lake, while in southwest region the beds were largely depleted. Filamentous algal cover was high in all but the southern region near North McMillan Creek, which is known to have one of the lowest levels of nutrients of any tributary entering Conesus Lake.

- In September, sampling sites in the north basin previously studied in 1968 and 2012 were surveyed by the rake toss method to determine species composition. The dominant species were coontail (*Ceratophyllum demersum*) and eelgrass (*Vallisneria americana*), while Eurasian watermilfoil (*Myriophyllum spicatum*) was dominant in the northernmost macrophyte bed, directly south of Vitale Park. Comparisons to the 1968 and 2012 studies showed a general decrease in milfoil dominance in all but the northern bed.

- Seasonal growth trends for milfoil-dominated macrophyte beds in the Graywood Gully, Sand Point, North Gully Cove and Cottonwood Gully areas showed that biomass culminated in August; when values peaked at weights of 300-400 g/m^2, which are close to historically high biomass levels.

- The surface area covered by the milfoil dominated beds was extremely low in some areas but moderate to high in other areas. Plants were almost completely absent below depths of 3-3.5 m compared to maximum depths of more than 6 m in the 1960's and 4 m in the 2009 survey. Macrophyte standing crops (Kg) followed the same relative trends as bed surface areas.

- Overall, Eurasian watermilfoil biomass appears to be on the decline relative to historical values. There was very little growth in the Sutton Point and Cottonwood Gully beds in 2020. In contrast, watermilfoil representation was above average at the Sand Point and North Gully Cove sites. Herbivory by the invasive Eurasian rudd fails explain these contradictory trends. We consider other possible explanations and recommend additional studies.

- We are beginning to explore the interactions between macrophyte beds and stream plume effluents. A preliminary report on these studies is presented in Appendix I.

- Cyanobacteria-dominated phytoplankton blooms are still a concern in Conesus Lake, but 2020 was a year of limited cyanobacteria prominence. This was evident in late season blooms of phytoplankton that were dominated by diatoms rather than cyanobacteria, as described in the study included in Appendix II.

II. Introduction

The macrophyte flora of Conesus Lake has been studied extensively, starting with the work of W.C. Muenschner in 1927. Muenschner judged several species to be predominant, including *Ceratophyllum demersum* (Coontail), *Elodea canadensis* (Waterweed), *Heteranthera dubia* (Water stargrass), *Myriophyllum* (probably *M. sibiricum*, Northern watermilfoil), *Najas flexilis* (Slender naiad) and 10 species of *Potamogeton* (Pondweeds). Muenschner's initial studies were not supplemented until Geneseo Professor Herman Forest and his co-workers conducted the first quantitative studies of the macrophyte community in Conesus Lake from 1967-1970. Forest and colleagues (1971, 1978) duplicated Muenschner's transects and sampled extensively throughout the lake, describing a diverse assemblage dominated by the very same species listed by Muenschner in 1927. The studies by Forest and colleagues were a response to concerns by stakeholders over the proliferation of macrophyte beds around the lake. Forest later inferred that these increases were due to the rise in dominance of the canopy forming invasive Eurasian watermilfoil (*Myriophyllum spicatum*)in Conesus Lake (Bosch 2012). Concerns about macrophytes waned until the late 1990's. Starting in 1994, after zebra mussel populations had spread throughout the lake, beds of watermilfoil and associated growth of filamentous algae became an impediment to lake use. In 1999, Bosch and colleagues (1999) were tasked with investigating the reasons for the renewed prominence of the macrophyte beds. They identified *M. spicatum* as the overwhelmingly dominant macrophyte in Conesus Lake. They also charted the regions where the largest macrophyte beds were located and found the densest watermilfoil beds adjacent to streams, where ample shallow habitat and consistent delivery of nutrients from stream runoff would promote growth of macrophytes as well as associated filamentous algal communities (Bosch *et al*., 1999). This observation was the impetus for the USDA Watershed Project, which began in earnest in 2000 and continued until 2009 when a special issue dedicated to the project was published in the *Journal of Great Lakes Research* (Makarewicz *et al*., 2009). Studies of macrophytes were completed by Bosch in subsequent years, but the last survey of Conesus Lake macrophytes was completed in 2012 (Bosch and colleagues 2012).

This 2020 study of the macrophyte communities in Conesus Lake continues a long-term program designed to monitor trends in the dominance and biomass of the invasive Eurasian watermilfoil. It has been 8 years since the macrophyte beds of the lake were studied comprehensively (Bosch and Colleagues, 2012). Anecdotal reports from lake residents in recent years indicate that macrophyte beds have been less prominent in recent years. Since that time the Eurasian Rudd (*Scardinius erythrophthalmus*), a fish species whose adults feed on macrophytes (Kapuscinski, 2012), have become very abundant in Conesus Lake, with schools exceeding 100 individuals now a common sight along the lake shore line. The impact of this species on the macrophyte beds is unknown.

III. Methods

This section describes the methodology for three different studies of the lake macrophyte community that were carried out in 2020:

1. On the 27th of July we conducted a lake-wide visual survey of the state of the main macrophyte beds. This survey additionally documented the extent of filamentous algal growth associated with the macrophyte beds.

2. On the 26th of September students of Geneseo's Aquatic Community course conducted a rake toss survey of selected sites in the north basin of the lakes. These were the sites sampled by Muenschner in 1926, Forest and colleagues in 1968, and Bosch and colleagues in 2012, to which the 2020 survey data are compared.

3. In addition to the two limited surveys described above, we also carried out a more detailed SCUBA diver and snorkeling study of macrophyte beds that were previously studied by Bosch and colleagues. For this study, quantitative surveys were carried out in June, July and August at Sutton Point and Cottonwood Gully in the southern region of the lake, North Gully Cove and Sand Point in the central part of the lake, and Graywood Gully in the northwest **(Figure 1).**

Lake-Wide Qualitative Survey

For the lake-wide survey carried out on July 27th, we recorded observations on the density and surface area coverage of the macrophytes in 24 locations on Conesus Lake. At each site we noted specifically the dominant species at each site and the extent of filamentous algal cover growing on the surface canopy of the macrophyte bed.

Rake Toss Survey of north basin sites

On the 26th of September a rake toss survey of selected sites in the north basin of the lakes was carried out. These were the sites sampled by Muenschner in 1926, Forest and colleagues in 1968, and Bosch and colleagues in 2012. Each sampled was bagged and frozen for later analysis. A few weeks later the samples were thawed, separated by species, blotted dry with paper towels and weighed. This is the blotted dry weight. To determine the actual dry weight of the sample, subsamples of the plants were pre-weighed, dried in an oven at 60 ºC for several days and then re-weighed. The percent of the initial sample that was dry weight was used to convert blotted dry weight to actual dry weight of tissue. The percent composition of macrophytes reported from this study was calculated from the dry weight data.

Comprehensive Survey of Macrophyte Bed Biomass

In addition to the two limited surveys described above, we also carried out a more detailed SCUBA diver and snorkeling study of macrophyte beds that were previously studied by Bosch and colleagues. For this study quantitative samples were collected in June (18th -25th), July (13th-15th) and August (10th-25th) for the macrophyte beds on Sutton Point and Cottonwood Gully in the southern region of the lake, North Gully Cove and Sand Point in the central part of the lake, and Graywood Gully in the northwest **(Figure 1).** Quantitative quadrat samples were collected by SCUBA divers along the same three transect lines and depths surveyed in previous years. The methods used to quantify macrophyte biomass are described in a previous technical report (Bosch *et al*., 2012). A more detailed account can be found in the published studies of the U.S.D.A. Watershed Study (Bosch *et al*. 2009).

To determine aquatic plant biomass, replicate quadrat samples (usually 3 at each depth) were collected at depths of 1, 2, and 3 m along three transects that were approximately the same as those used in previous studies. A 0.5m x 0.5m quadrat constructed from PVC pipe was placed on the bottom and all shoot biomass was harvested by hand. Each sample was placed in a numbered plastic collection bag and taken to the laboratory for species sorting and zebra mussel removal. Plant species within each sample were blotted dry with paper towels and weighed separately to the nearest 0.1g with an electronic scale. The blotted dry weights were used for all analysis in this study.

The surface area of the macrophyte beds and the milfoil-dominated area of the beds were mapped at each site using global positioning systems (GPS). To record points, a Garmin was used by an individual aboard a boat while a swimmer indicated points to be mapped around the perimeter of milfoil dominated areas in each bed. ArcGIS software was used to analyze these maps for surface area. Multiple independently surveyed maps were made for several of the sites to assess the precision of our measurements.

Standing crop in Kg total weight was calculated for each site by multiplying the average quadrat biomass for the 2-3 m samples dominated by watermilfoil times the surface area of the milfoil dominated area.

IV. Results and Discussion

Lake-Wide Qualitative Survey

This one-day survey of the whole lake confirmed that some of the Eurasian watermilfoil dominated beds in Conesus Lake continue to thrive, while in other areas the populations are significantly depleted (**Table 1**). By the time of our survey on July 27, watermilfoil plants were beginning to canopy at Sand Point and they were not far behind in Wilkins Cove, McPhersons Cove (North of McPhersons Point), North Gully Cove (South of McPhersons Point) and Graywood Gully (**Figure 2**). In contrast to these areas of prominent growth, macrophyte beds in the southwest region of the lake that were previously dominated by Eurasian watermilfoil, were nearly devoid of such growth.

These included the areas of Sutton Point, Cottonwood Gully and Long Point Cove, where isolated watermilfoil plants or low growing patches of plants could be seen, but biomass was a small fraction of what is documented for these sites as recently as 8 years ago. Milfoil beds typically overwinter as degraded shoots and regrow rapidly in spring, as clearly happened for many in the North Basin this past year, but every few years there is more extensive decay and plants overwinter as roots. That may be what has happened to the milfoil in the southwest region of the lake. The cause of the "die-back" is unknown, but we have observed this phenomenon in previous years and found that by the second season after the event the beds had returned to their normally vigorous growth.

The biomass of filamentous algae was extensive in most of the lake. Eurasian watermilfoil continues to serve as an excellent substrate for these algae (**Figure 2**). Even in the absence of watermilfoil, algae were seen growing on eelgrass and other macrophytes and over the bottom, where we observed large clumps of filamentous algae. The most extensive growth was seen near streams such as Hanna's Creek, Wilkins Creek, Densmore Gully, North Gully, Long Point Gully, Sand Point Gully, Eagle Point Gully and Graywood Gully. Rapid growth of filamentous algae is often the result of phosphorus runoff from the watershed (D'Aiuto *et al.* 2006). In spring 2020 there were several major rain events, and we believe that nutrients from these events were responsible for the prolific growth of filamentous algae in 2020. Another observation that points to external loading as a factor is that the lowest qualitative biomass of filamentous algae was seen near North McMillan Creek, a stream that historically has among the lowest nutrient concentrations of any tributary entering Conesus Lake.

Rake Toss Survey of North Basin Sites

Seven different species of macrophytes were identified in the six sites studied in the North Basin: *Myriophyllum spicatum* (Eurasian milfoil), *Ceratophyllum demersum* (Coontail), *Vallisneria americana* (Water celery/Eelgrass), *Ruppia sp.* (Ditch grass), *Najas flexilis* (Slender Naiad), *Heteranthera dubia* (Water stargrass) and *Scirpus subtermianlis* (Water bulrush). Among the seven, the three prominent species in order

of relative dry weight (greatest to least) were Eurasian milfoil, coontail and eelgrass (**Figure 3A, Table 2**). Across the six sites sampled, two were dominated by Eurasian milfoil (**Figure 3A**). At Sand Point North (area south of Vitale Park) milfoil comprised over 50% of the dry weight biomass and at Graywood Gully it was 76% of the biomass. In contrast, the other four sites, Wilkins creek, Old Orchard Cove, Eagle Point, and Pebble Beach, all had less than 20% dry weight composition comprised of Eurasian milfoil (Old Orchard Cove 11%, Eagle Point 13%, Wilkins Creek 15% and Pebble Beach 17%). Eelgrass was the dominant species at Wilkins Creek and Old Orchard Cove, whereas coontail was the most abundant at Eagle Point and Pebble Beach.

While it is true that the 2020 rake sampling was very limited, we draw a few general conclusions from our study of the north basin historical sites. Overall, when compared to the previous studies of Forest (1968) and Bosch *et al.* (2012), the macrophyte community has changed substantially; Eurasian milfoil has declined in relative abundance at most sites (**Figure 3B**). North basin-wide, Eurasian milfoil remains the most abundant species, but this trend was due to its high dominance at two of the sites (Graywood and Sand Point North), where large milfoil beds have been reported previously (Bosch *et al.*, 2009, 2012). Another species, Water stargrass (*Heterantheria dubia)*, has decreased in abundance since the earliest studies. Eurasian watermilfoil became dominant in Conesus Lake during the late 1960's. It occupies the same general habitat as Water stargrass in the 1.5-3 m depth range and apparently Water stargrass was outcompeted by the expanding milfoil. By the time Bosch and colleagues conducted their studies from 2001 to 2012, Water stargrass had a limited abundance, having been reduced to dominance in just a few areas of the lake (Bosch *et al.*, 2012). Consistent with this long-term trend we found almost no Water stargrass in our samples.

Quadrat Biomass, Surface Area and Standing Crop

Here we report the results of quadrat sampling and mapping studies conducted by SCUBA diving and snorkeling from late June to late August, 2020. The trends documented for 2020 are compared to an extensive historical record dating back to

2000 for the study sites referred to as Graywood Gully, Sand Point, North Gully Cove, Cottonwood Gully and Sutton Point.

In general terms, we found that high densities of Eurasian watermilfoil biomass in excess of 200 g dry wt./m^2 persisted at depths of 1-3 m in the central and northern lake sites (Graywood Gully, Sand Point and North Gully Cove) **(Figure 4, Table 3).** The densest milfoil-dominated region was located in the southernmost sections of the Graywood Gully bed, where biomass in excess of 400 g dry wt./m^2 was typical in August. In contrast to the high watermilfoil densities in the central and northern beds, the Sutton Point and Cottonwood Gully sites along the southwest region of the lake had only small patches of watermilfoil and the density in these patches was consistently below 200 g dry wt./m^2. It is worth noting that in other areas of the south basin (e.g., Long Point Cove, Harston Point) the watermilfoil was also historically sparse.

Samples were collected in June, July and August to document the seasonality of biomass accumulation in the watermilfoil dominated regions. Our data indicate quite clearly that biomass peaked in August and there is evidence that the maximum growth rates for milfoil occurred between the mid July and mid-late August sampling dates (**Figure 4**, ANOVA $p < 0.05$)

Much like the trends in milfoil per m^2 for Sutton Point and Cottonwood Gully, we found that the areas covered by milfoil at these sites were greatly diminished. As shown in **Table 4,** the respective surface area of these beds was 6% and 4% of the long term average (See also long term data set in **Table 5**). In fact, for most of the summer season there was little milfoil to be seen at Sutton Point and Cottonwood Gully. It was only in August that we began to see some patches of plants that covered small areas of 343 and 269 m^2 , whereas the average size of these beds from 2000-2012 was 27 times and 17 times higher (**Table 4, 5**)

In the Graywood Gully and North Gully Cove areas, watermilfoil was somewhat diminished compared to the long term averages (see **Tables 4 and 6**), but at 9,780 and 8,920 m^2 still covered very large areas of the 1-3 m bottom (See **Figure 5**). In the Graywood Gully area, the northern portion of the macrophyte bed is historically quite variable in coverage and milfoil composition. That same pattern was observed this year (**Table 7**). Despite covering nearly 9 thousand m^2, the North Gully Cove bed

continued a pattern of decline first observed in 2010 (**See Table 6**). We identified two reasons for these diminished proportions. First, the milfoil biomass in the shallow areas is very patchy, with only a few areas having significant growth. Second, we saw virtually zero plant biomass below the depth of 3 m at this site, whereas growth extended to a depth of 4 m in previous studies (Bosch *et al*., 2009)

Our impression is that the Sand Point macrophyte bed stood out in terms of having consistently high density over a very broad area. The surface area of this bed was measured three different times (See **Figure 5**), yielding an average and standard deviation of 9,153 $\pm$ 996 m^2. The maximum areal measurement in 2020 was 9,857 m^2, which was the highest recorded in 10 years of sampling. As in all our other study sites, there was little or no growth below 3 m at Sand Point, so we suspect that the increased surface of the milfoil bed is due to more extensive growth in the shallow region of the habitat. The coefficient of variation (S.D/mean *100) for these three replicate mapping efforts was slightly high at 10.9 (**Figure 5**), However, the coefficients of variation for the Graywood Gully and North Gully Cove beds were both 6.3 (**Table 4, Figure 5),** which indicates a strong level of precision and confidence in the reliability of all our mapping surveys.

By multiplying the average plant biomass density in the 2-3 m zone times the surface area of coverage we were able to estimate the standing crop of each bed. The long term record of standing crops (as well as biomass density and bed surface area) for each of our study sites are shown in **Tables 5, 6 and 7**. Graphs depicting trends in biomass per m^2 and total standing crop in Kg can be found in **Figures 6, 7 and 8**. The sites are located in different areas representing almost all portions of the lake (See **Figure 1**). We can see from these data that the standing crop for Sand Point (central lake) was moderate to high compared to the long term record, and North Gully (central lake) and Graywood Gully (northwest lake; **Figure 9**) were moderate to low. The Cottonwood Gully and Sutton Point macrophyte beds located in the southern section of Conesus Lake had exceptionally low growth of macrophytes in what are typically Eurasian watermilfoil dominated areas.

V. Conclusions

The macrophyte community of Conesus Lake had not been studied systematically since 2012. The primary goal of the present study was to determine if Eurasian watermilfoil populations had declined since 2012, as reported by many residents. Additionally, we hoped to gain insights as to whether herbivory by the invasive Eurasian rudd could account for the reduction in biomass reported.

We found that dense Eurasian watermilfoil beds with very high biomass persisted in several areas of the lake very much as they had for at least the last 20 years. Specifically, the Sand Point, North Gully Cove and Graywood Gully long term study sites continued to be dominated by dense populations of this invasive plant. In contrast, vast areas of the southern basin of the lake (as represented by the Sutton Point region, the Cottonwood Gully region and the Long Point Cove region) that were once densely populated by Eurasian watermilfoil, were in 2020 nearly devoid of growth.

These contradictory trends are difficult to explain as the result of a single ecological factor such as increased herbivory due to the Eurasian rudd. A more plausible explanation is that the southern region beds decayed during the winter of 2019-2020 and survived only as roots that did not fully repopulate the macrophyte community in the first growing season. We have observed this phenomenon in previous years. If so, we might expect the southern basin beds to have fully recovered by the end of summer 2021. In the northern portion of the lake the beds may have survived the winter as shoots that then rapidly replenished the northern basin biomass during the summer 2020. A limited follow up study in 2021 would help our understanding of the current growth dynamics of Eurasian watermilfoil in Conesus Lake.

VI. Acknowledgements

We would like to express our gratitude to a number of people who continue to help us accomplish the goals of the summer monitoring program: SUNY Geneseo's Biology Department and especially Ed Beary and Yvonne Mehlenbacher; Dr. Anne Baldwin and Betsy Colón of Geneseo's Office of Sponsored Research; Gene Bolster and the members of the Conesus Lake Association; and Heather Ferrero and Mary Underhill of the Livingston County Planning Department. This research project was funded by a grant from Finger Lakes -Lake Ontario Watershed Alliance administered by the Department of Environmental Conservation and the Livingston County Planning Department.

VII. Literature Cited

Bosch, I., J. Makarewicz, P. Thorn and M. Martin. 1999. Distribution and Standing Crops of Submersed Macrophytes in Conesus Lake, N.Y. . Report to the Livingston County Planning Department, 49 pp.

Bosch, I. J., Makarewicz, J.C., Lewis, T.W., Bonk, E.A., Romeiser, J., and Ruiz, C. 2009. Responses of macrophytes beds dominated by Eurasian milfoil (*Myriophyllum spicatum*) to decreases in nutrient loading from managed agricultural watersheds: Declines in biomass. *J. Great Lakes Res.* #35: 90-98

Bosch, I., H. Dodge, A. Dumas and M. Stryker. 2009. Continued Monitoring of Macrophyte Biomass and Filamentous Algal Cover in Conesus Lake. Report to the Livingston County Planning Department, 23 pp.

Bosch, I, T. Shuyskey, S.M. Snyder and A. Brodsky. 2012. Historical Trends of Macrophyte Diversity and Biomass in Conesus Lake (Summer 2012)

D'Aiuto, P.E., Makarewicz, J.C., and Bosch, I. 2006. The impact of stream nutrient loading on macrophytes and metaphyton in Conesus Lake, USA. *Verh. Internat. Verein. Limnol*. 29:1373-1376.

Forest, H.S. and E.L. Mills. 1971. Aquatic flora of Conesus Lake. *Proc. Rochester Acad. Sci.* # 12, pp 110-138.

Forest, H.S., J.Q. Wade and T.F. Maxwell. 1978. The limnology of Conesus lake. In Lakes of New York State. Vol. I. Ecology of the Finger Lakes. J.A. Bloomfield, Ed. Academic Press, N.Y. pp. 122-221.

Kapuscinski, F. (2012). Feeding patterns and population structure of an invasive cyprinid, the rudd Scardinius erythrophthalmus (Cypriniformes, Cyprinidae), in Buffalo Harbor (Lake Erie) and the upper Niagara River. *Hydrobiologia,* 693(1), 169–181.

Makarewicz, J.C., Lewis, T.W., Bosch, I., Noll, M., Herendeen, N., Simon, R., Zollweg, J., and Vodacek, A. 2009. The impact of agricultural best management practices on downstream systems: Soil loss and nutrient chemistry and flux. *J. Great Lakes Res*. 35:23-36

Muenschner. W.C. (1927). Vegetation of Silver Lake and Conesus Lake. In "A Biological Survey of the Genesee River Watershed". Supplement to Annual Report No. 16, pp. 66-71, and Appendix VII, pg. 86. N.Y. State Department of Environmental Conservation, Albany.

Tables

Table 1. Observations of macrophyte biomass and filamentous algal cover from one day lake-wide survey (August 4, 2020).

	Location	Nearest Stream	Milfoil Growth	Algal Cover	Comments
	North, Northeast Lake				
1A	No. by Vitale Park	Hanna's Creek	Sparse or none	Heavy	Algae on bottom, on eelgrass, milfoil
1B	No. End Center 2m	No nearby creek	Low milfoil	Negligible	At 2m, low milfoil bed, not much algae
2A	North of Wilkins Creek	Wilkins	Sparse or none	Heavy	Eelgrass dominated
2B	Wilkins Cove No.	So. Wilkins Cr.	Sparse to none	Heavy	Eelgrass covered in algae
2C	Wilkins Cove Cent.	Center of Cove	Present, low	Heavy	Milfoil not very tall; eelgrass as well
2D	Wilkins Cove South 2m	Far South Wilkins Creek	Present, low	Heavy	Low milfoil & eelgrass; moderate cover
3A	Stella Maris (N. of Camp)	Small Creek to North	Sparse or none	Negligible	North of Stella Maris not much growth
3B	South of Stella Maris	Creek as above	Dense, mid water	Heavy	Milfoil smothered by algae
4A	Old Orchard Pt. at Gully	Densmore Gully	Dense but low	Heavy	Milfoil smothered by algae
4B	McPhersons Cove Center	Small culverts/pipes	Very Dense, mid ht.	Heavy	Large milfoil bed, high algal cover
	Southeast, South Lake				
5A	McPhersons Point	North Gully	Patchy	Moderate	North Gully milfoil bed
5B	North Gully Cove	North Gully	Dense milfoil	Heavy	At 1.5 – 3m; sparse growth
5C	North Gully Cove (South)	North Gully	Dense milfoil	Heavy	At 1.5 – 3m; not much growth near docks
6	Harston Pt. N of Gully	Harston Pt Gully	Moderate	Moderate	Some milfoil w/ algal cover
7	Walkley's Land./Dacola Sh.	North McMillan	Moderate	Negligible	Clear area- mixed milfoil/eelgrass w/o algae
	Southwest Lake				
8	Maple Beach	Southwest Creeks	Sparse/none	Moderate	Very deep area near gully; not much plant life
9A	Sutton Point South	Sutton Point Gully	Sparse/none	Negligible	Dense milfoil bed once; today mostly eelgrass
9B	Sutton Point Center	At Sutton Pt. Gully	Sparse	Negligible	Dense milfoil bed once; today mostly eelgrass
9C	Sutton Point North	Sutton Point Gully	Moderate	Negligible	Milfoil to the north but only a fraction of old
10	Long Point Cove	LP Cove Gully	Sparse	Moderate/Heavy	Bottom algae; little milfoil in once dense bed
	Northwest Lake				
11	Long Point	Long Point Gully	Dense	Heavy	As in the past a dense bed but more algae
12	Sand Point	Sand Point Gully	Densest	Heaviest	Extreme conditions
13	Eagle Point	Eagle Point Gully	Dense	Heavy	Plant growth north of gully
14	Grayshores	Grayshores Gully	Dense	Heavy	Dense plant growth north and south of the Gully

Table 2. Summary of macrophyte percent species composition for all five north basin sites surveyed during September 2020. The comparison is based on dry weight conversions.

North Basin Sites			
Species Name	**Common Name**	**Total g DW**	**% of Total Dw**
Myriophyllum spicatum	Eurasian milfoil	283.2	46.8
Ceratophyllum demersum	Coontail	180.3	29.8
Vallisneria Americana	Wild Celery/Eelgrass	114.1	18.9
Najas flexilis	Slender naiad	0.1	0.0
Heteranthera dubia	Water stragrass	15.3	2.5
Scirpus subterminalis	Water bullbrush	2.2	0.4
Ruppia sp.	Ditch Grass	9.5	1.6
	Total g DW in Quadrats	**604.5**	**100.0**

Table 3. Biomass quadrat data for 1, 2 and 3 m depths of each bed. Blotted wet weight average and standard deviations are shown for each sampling date in June, July and August 2020.

Milfoil Bed Location		**June Mean ± S.D.**	**July Mean ± S.D.**	**August Mean ± S.D.**
Graywood	**1 m**	28 ± 35	No Milfoil	No Milfoil
Gully	**2 m**	88 ± 55	84 ± 58	437 ± 257
Quadrats	**3 m**	50 ± 35	116 ± 42	260 ± 192
Sand Pt.	**1 m**	123 ± 56	204 ± 135	No milfoil
Gully	**2 m**	229 ± 140	195 ± 59	393 ± 106
Quadrats	**3 m**	224 ± 89	168 ± 73	311 ± 123
North	**1 m**	132 ± 85	357 ± 108	No milfoil
Gully	**2 m**	148 ± 18	145 ± 134	374 ± 105
Quadrats	**3 m**	48 ± 22	204 ± 26	236 ± 80
Cottonwood	**1m**	55 ± 68	No Milfoil	No Milfoil
Gully	**2 m**	148 ± 18	140 ± 86	178 ± 33
Quadrats	**3 m**	No plants	No plants	No plants
Sutton Pt.	**1 m**	No plants	No plants	No plants
Gully	**2 m**	No plants	No plants	210 ± 121
Quadrats	**3 m**	No plants	No plants	No plants

Table 4. Comparisons of milfoil bed surface area at the five principal long term monitoring sites in Conesus Lake. The mean, standard deviation and the coefficient of variation (CV = standard deviation/ average) are shown for replicate measurements made in 2020.

Milfoil Bed Location	Milfoil Bed Cover (m^2)				
	Long Term Average	**Long Term Range**	**2020 Avg. ± S.D. & CV**	**2020 Maximum**	**% of Long Term Average**
Graywood Gully	18,648	6,703 - 26,864	9,359 ± 596 *CV = 6.3*	9,780	52
Sand Pt. Gully	7,799	3,846 - 9,781	9,153 ± 996 *CV = 10.9*	9,857	126
North Gully	20,552	13,325 - 30,099	8,347 ± 530 *CV = 6.3*	8,920	43
Cottonwood Gully	6,451	2,283 - 9,387	238 ± 43	269	4
Sutton Pt. Gully	5,891	3,688 - 13,802	343	343	6

Table 5. Historical record of macrophyte average biomass, milfoil-dominated bed surface area and total macrophyte standing crop at the two long term research sites on the South region of Conesus Lake.

Location	Year	Average Biomass grams . m^2	Surface Area m^2	Standing Crop Kg Dry Wt.
Sutton Point Gully	2000	184 ± 43	---	---
	2001	467 ± 183	8,592	4,017
	2002	71 ± 40	3,688	262
	2003	138 ± 92	11,819	1631
	2004	227 ± 77	11,909	2,703
	2005	197 ± 90	11,995	2,349
	2006	364 ± 208	7,438	2,707
	2007	295 ± 94	10,973	3,232
	2008	190 ± 106	5,985	1,201
	2009	224 ± 112	13,802	3,099
	2010	135 ± 47	7,390	998
	2012	270 ± 57	6,610	1,785
	2020	210 ± 121	343	72
Cottonwood Gully	2000	193 ± 85	---	---
	2001	373 ±168	9,387	3,501
	2002	316 ± 134	7,360	2,326
	2003	146 ± 43	3,750	548
	2004	234 ± 41	9,205	2,154
	2005	273 ± 81	6,880	1,878
	2006	283 ± 61	5,605	1,589
	2007	155 ± 140	8,100	1,253
	2008	-	-	-
	2009	135 ± 78	4,860	657
	2010	252 ± 90	7,077	1783
	2012	154 ± 107	2,283	352
	2020	148± 18	269	40

Table 6. Historical record of macrophyte average biomass, milfoil-dominated bed surface area and total macrophyte standing crop for beds around the central region of Conesus Lake, south of McPhersons Point (North Gully) and on Sand Point.

Location	Year	Average Biomass grams . m^2	Surface Area m^2	Standing Crop Kg Dry Wt.
North Gully	**2000**	**262 ± 134**	**23,192**	**6,192**
	2001	**459 ± 202**	**25,783**	**11,834**
	2002	**151 ± 74**	**12,004**	**1,813**
	2003	**304 ± 176**	**19,760**	**6,007**
	2004	**186 ± 57**	**30,099**	**5,598**
	2005	**188 ± 105**	**21,798**	**4,098**
	2007	**225 ± 70**	**27,850**	**6,266**
	2008	**266 ± 167**	**11,855**	**3,149**
	2009	**283 ± 108**	**24,267**	**6,874**
	2010	**265 + 175**	**13,325**	**3,531**
	2012	**272 + 153**	**14,133**	**3,844**
	2020	**313 + 72**	**8,920**	**2,792**
Sand Point Gully	**2000**	**212 + 29**	**9,535**	**2,021**
	2001	**484 + 300**	**9,781**	**4,730**
	2002	**325 + 82**	**7,354**	**2,390**
	2003	**290 + 126**	**5,310**	**1,540**
	2004	**131 + 34**	**8,474**	**1,110**
	2005	**191 + 96**	**8,349**	**1,595**
	2006	**230 + 92**	**9,775**	**2,246**
	2007	**112 ± 111**	**9,684**	**1,084**
	2008	**201 ± 71**	**6,022**	**1,147**
	2009	**222 ± 111**	**6,564**	**1,457**
	2010	**205 + 19**	**4,939**	**1,012**
	2012	**301 + 146**	**3,846**	**1,158**
	2020	**347 + 120**	**9,857**	**3,420**

Table 7. Historical record of macrophyte average biomass, milfoil-dominated bed surface area and total macrophyte standing crop for Graywood Gully. This area has been sampled less frequently in recent years. Overall, the average biomass was relatively high in 2020 but the surface area and standing crop were low because milfoil and other macrophytes have declined from the northern portions of this bed.

Location	Year	Average Biomass grams . m^2	Surface Area m^2	Standing Crop Kg Dry Wt
Graywood Gully	**2000**	**238**	**---**	**---**
	2001	**412 ± 162**	**---**	**---**
	2002	**193 ± 123**	**6,703**	**1,294**
	2003	**131 ± 79**	**14,186**	**1,858**
	2004	**190 ± 54**	**26,864**	**5,104**
	2005	**230 ± 101**	**23,988**	**5,517**
	2006	**91 ± 37**	**21,843**	**1,982**
	2007	**168 ± 75**	**27,170**	**4,572**
	2020	**233 ± 130**	**9,780**	**2,279**

Figures

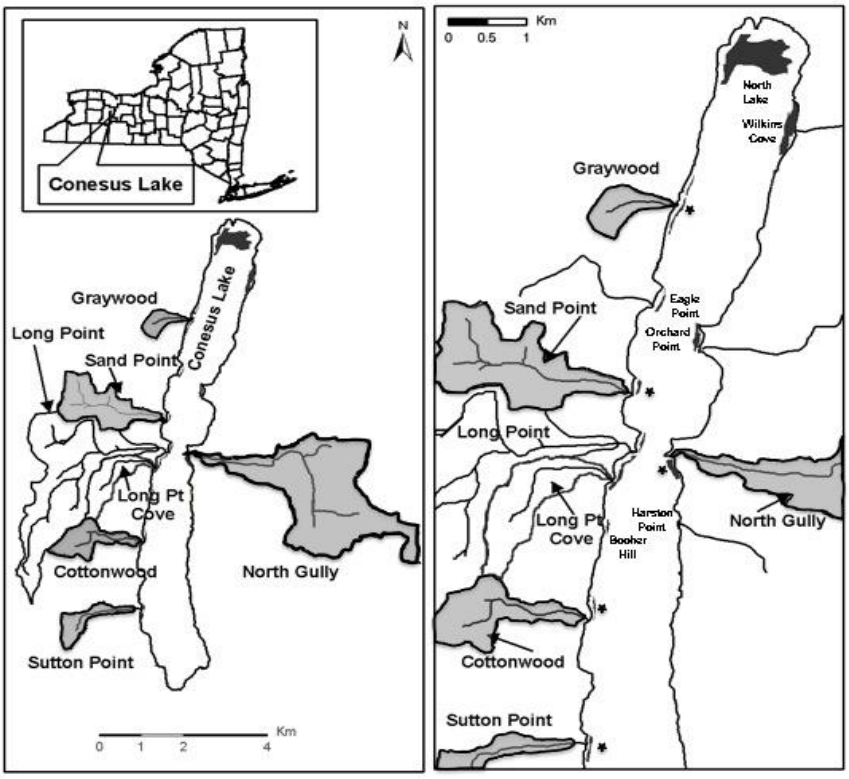

Figure 1. Map showing some of the largest macrophyte beds in Conesus Lake in their geo-referenced positions. Aras studied in 2020 are identified by a star symbol. The sub-watersheds and streams associated to the five sampling sites are shaded.

Figure 2. Images showing watermilfoil plants and associated filamentous algal growth (green stringy material) near several streams. From left to right : Wilkins Cove south of Wilkins Creek; near North McMillan Creek showing brown coloration more typical of macrophytes; North of Sand Point Gully ; North of Graywood Gully.

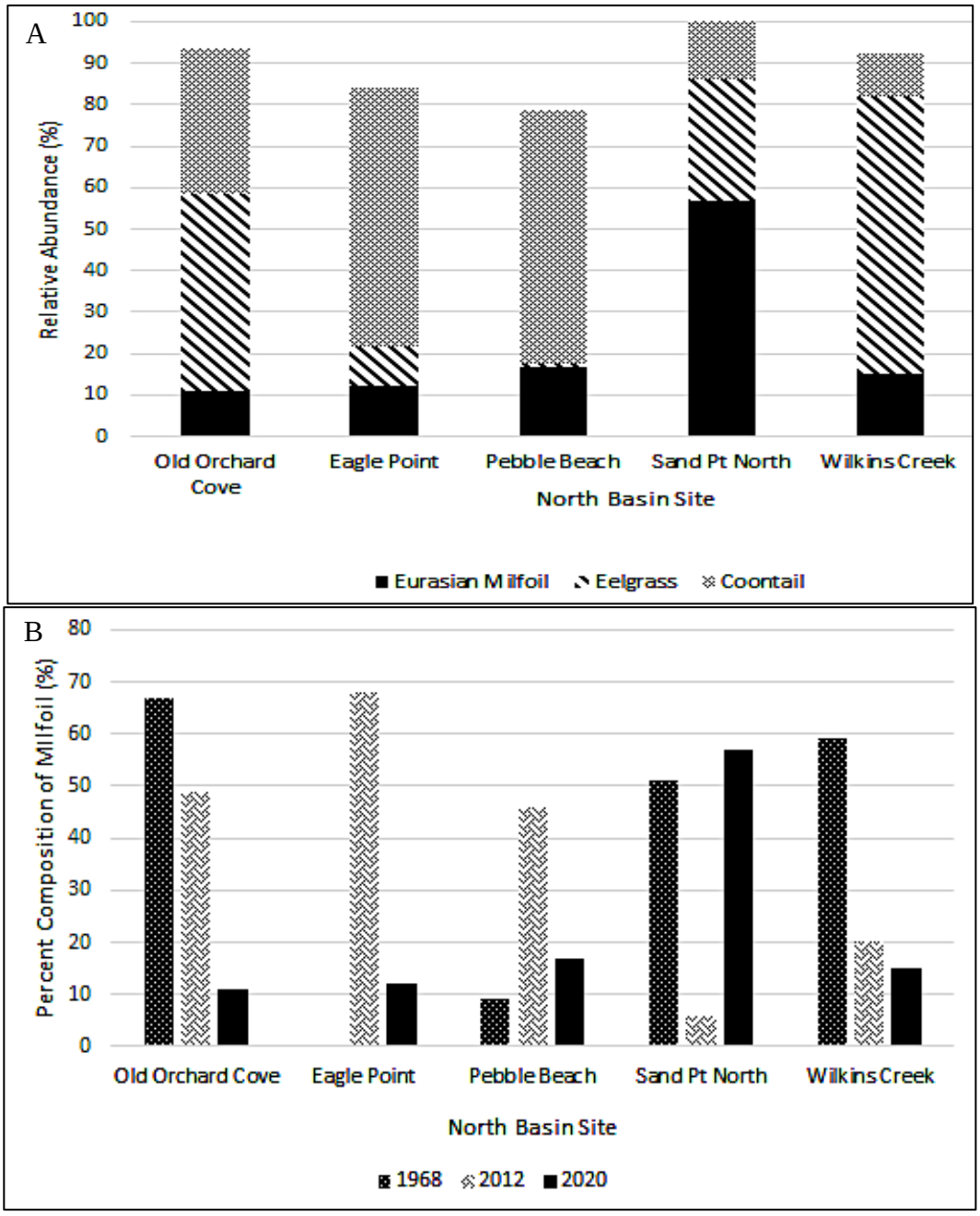

Figure 3. September survey of watermilfoil dominance at five locations in the North Basin that have been sampled previously by SUNY Geneseo researchers (Herman Forrest 1968, Isidro Bosch 2012). Top: Relative abundance of Eurasian watermilfoil in 2020 Bottom: Milfoil percent composition compared for 1968, 2012 and 2020. Comparisons are based on biomass dry weight.

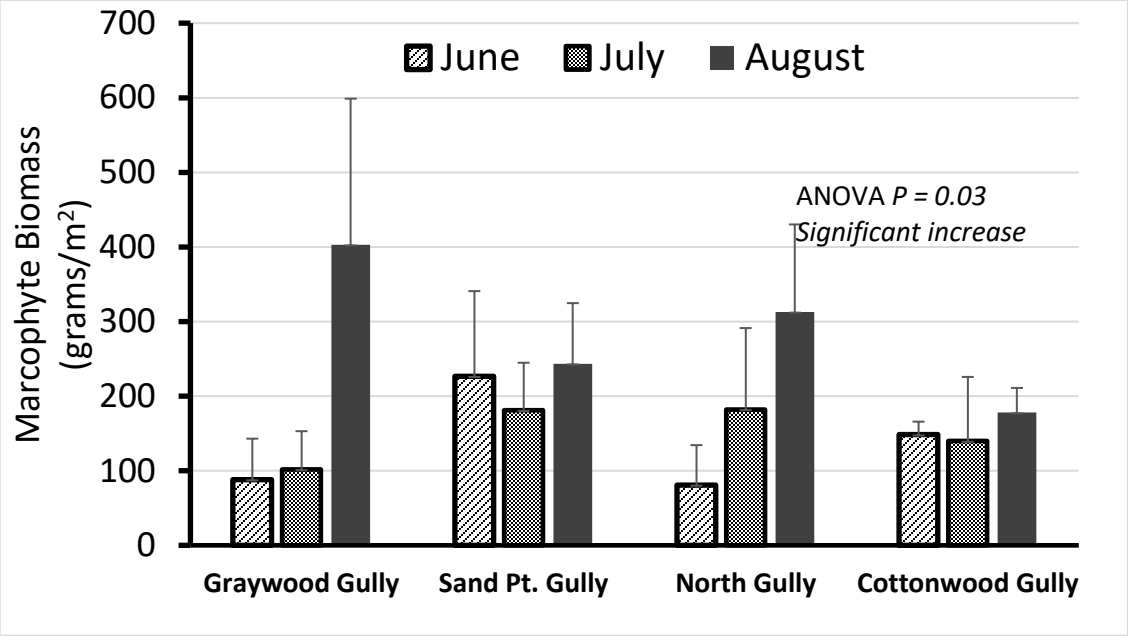

Figure 4. Seasonal changes in biomass of macrophytes as blotted wet weight between June and August sampling dates in 2020. The Sutton Point Gully macrophyte bed is not included in this comparison because only a small patch of milfoil was found at this site in August.

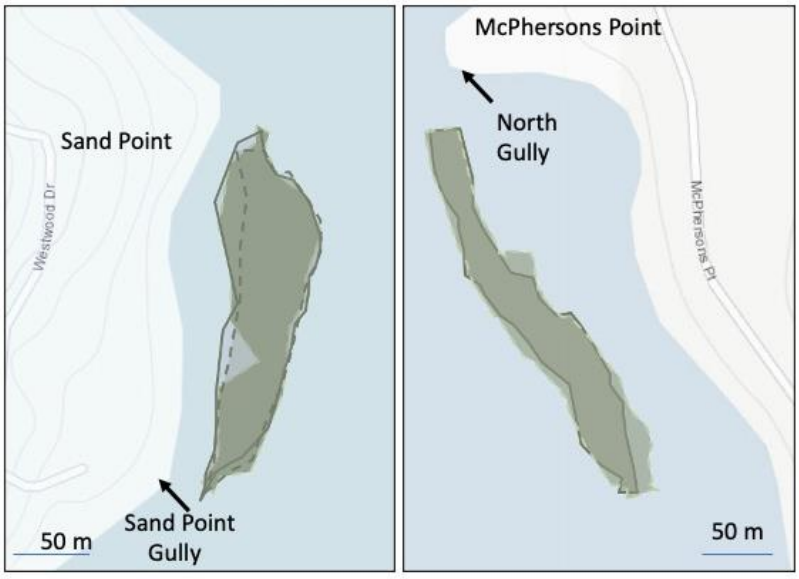

Figure 5. Maps of the Sand Point Gully and North Gully milfoil dominated beds. Replicate measures of surface area coverage were made by tracking the perimeter of each bed (defined as >25% milfoil shoots). Precision is most difficult along the inner margin of the beds where the milfoil edge is more irregular and at times difficult to define. The coefficient of variation in bed surface area was 10.9 for Sand Point and 6.3 for the bed in North Gully cove. See Table 4 for detailed numerical data.

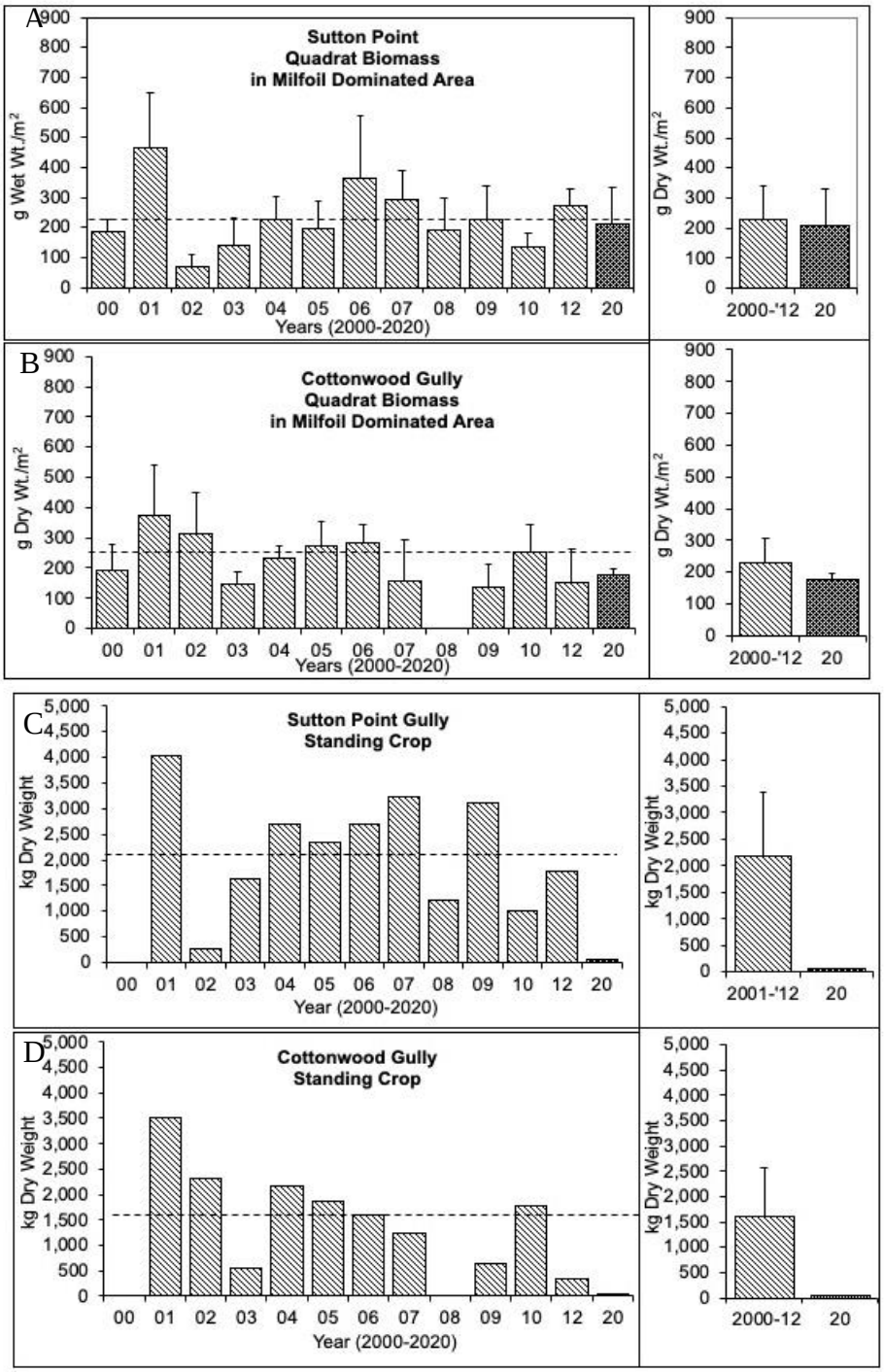

Figure 6. Long term trends in quadrat biomass (A and B) and standing crop (C and D) for the Sutton Point Gully and Cottonwood Gully sites in the southern region of Conesus Lake. Data trends show consistent biomass but a decline in standing crop culminating in extremely low values for 2020. These declines in standing crop are the result of the decreasing area of the beds (See Table 4).

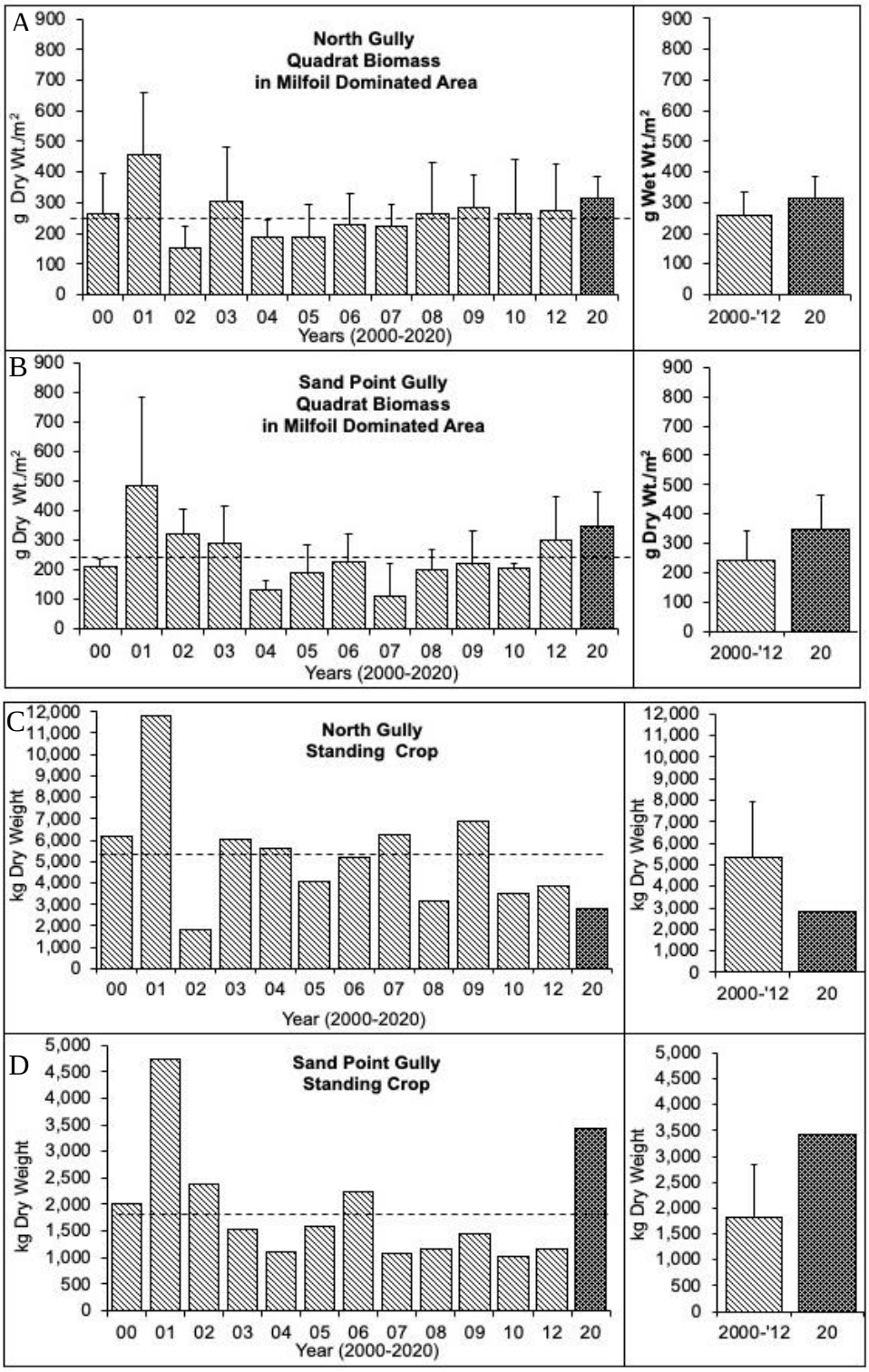

Figure 7. Long term trends in quadrat biomass (A and B) and standing crop (C and D) for the North Gully and Sand Point sites in the central region of Conesus Lake. Data trends show that biomass has been consistent at these sites for some time. Standing crop was low for 2020 at the North Gully site, but high at Sand Point Gully, due to both elevated biomass and high surface area of the bed (See Table 4).

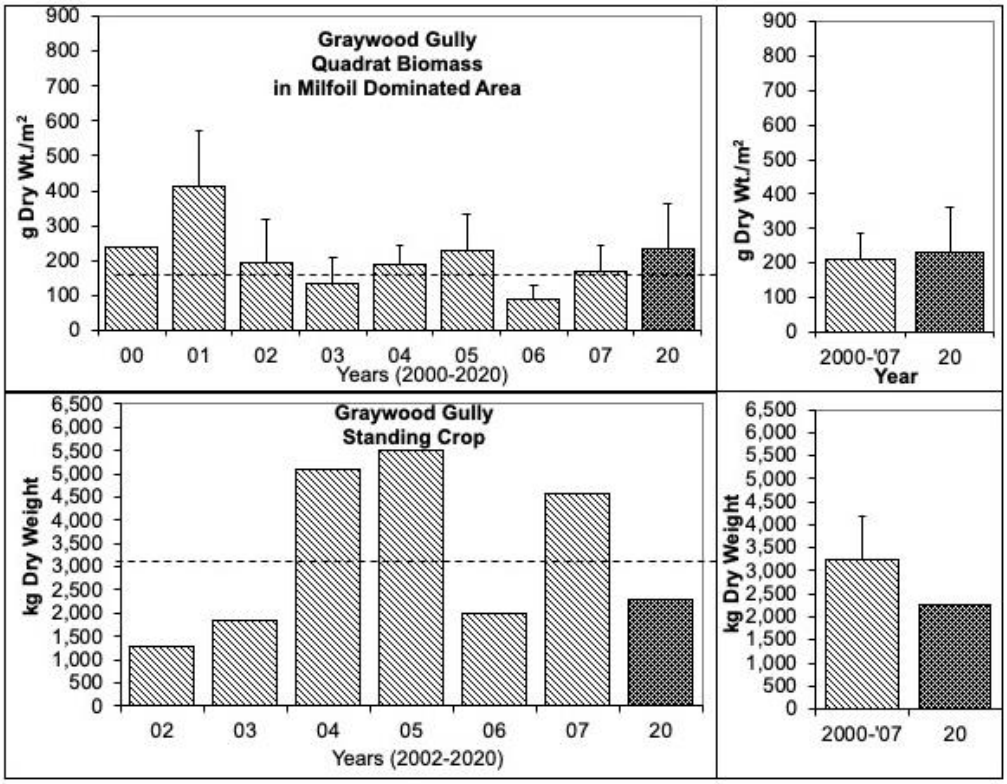

Figure 8. Long term trends in quadrat biomass and standing crop for the Graywood Gully macrophyte bed, which is located in the northwest region of the lake. Most of the biomass is located along the southern region of the bed. Northern portions furthest from the stream fluctuate in milfoil cover and that accounts for the variation in standing crop over the few years sampled.

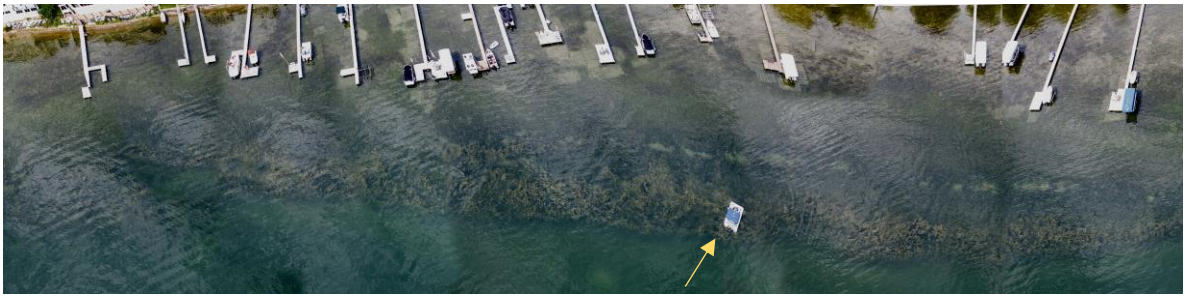

Figure 9. Southern portion of the Graywood Gully macrophyte bed shown in an image taken by a drone. The Graywood Gully tributary drains approximately 175 m to the north (right) of the 20 ft research boat at the bottom of the image (arrow).

Appendix I. Tributary Plume Study

Tributary Plume Dispersion Patterns: Observations from Aerial Surveillance and *In Lake* Conductivity Sensors

by Karl Hanafin, Isidro Bosch and Michael Chislock

A study of the impact that macrophyte beds have on the distribution of nutrients entering Conesus Lake by tributaries was conducted this past summer. The research approach was to develop and deploy five conductivity sensors around the macrophyte beds directly offshore from Graywood Gully. The objective was to measure differences in the water conductivity inshore and offshore of the macrophyte bed as rain events introduced significant quantities of water with high concentrations of dissolved nutrients. By measuring the response of conductivity to a series of rain events over the macrophyte growing season, it might be possible to assess the physical impact of the macrophyte bed on intercepting nutrients in the nearshore.

The sensor locations with respect to the tributary and the position of the macrophyte bed are shown here (small numbers identify the sensor number, dashed line represents the approximate position of the macrophyte bed):

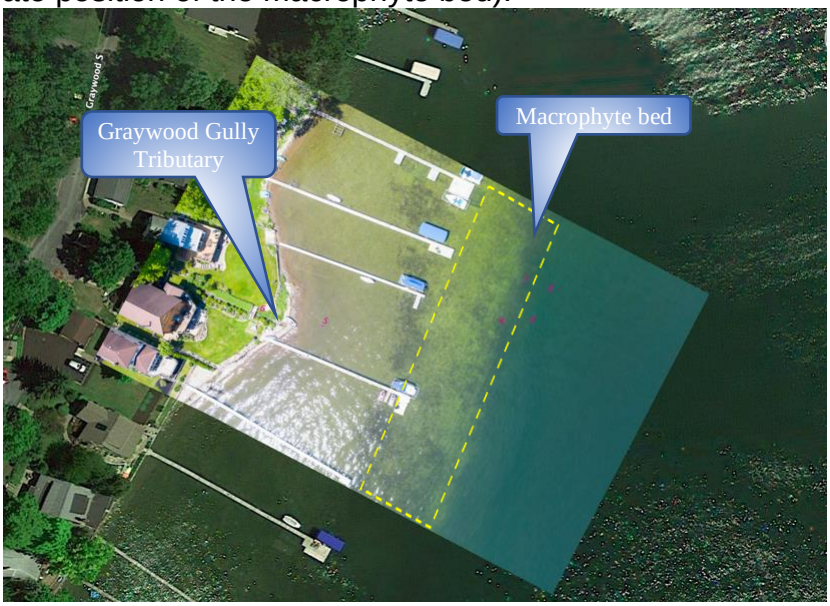

The sensor design was calibrated for the range of interest and consistently provided results well within 10% of reference solutions expected results. The sensors were tested after being removed from the lake with similar results. The systems minimum step value is approximately 0.002 mS/cm and consistently responded to changes in conductivity of 0.005 mS/cm.

One of the more significant rain events of this summer occurred on July 11, 2020. In excess of 2 inches of rain fell between 4:00pm and 9:00pm as measured by a local

automated rain gauge. The relevant conductivity and water temperature data is graphed below:

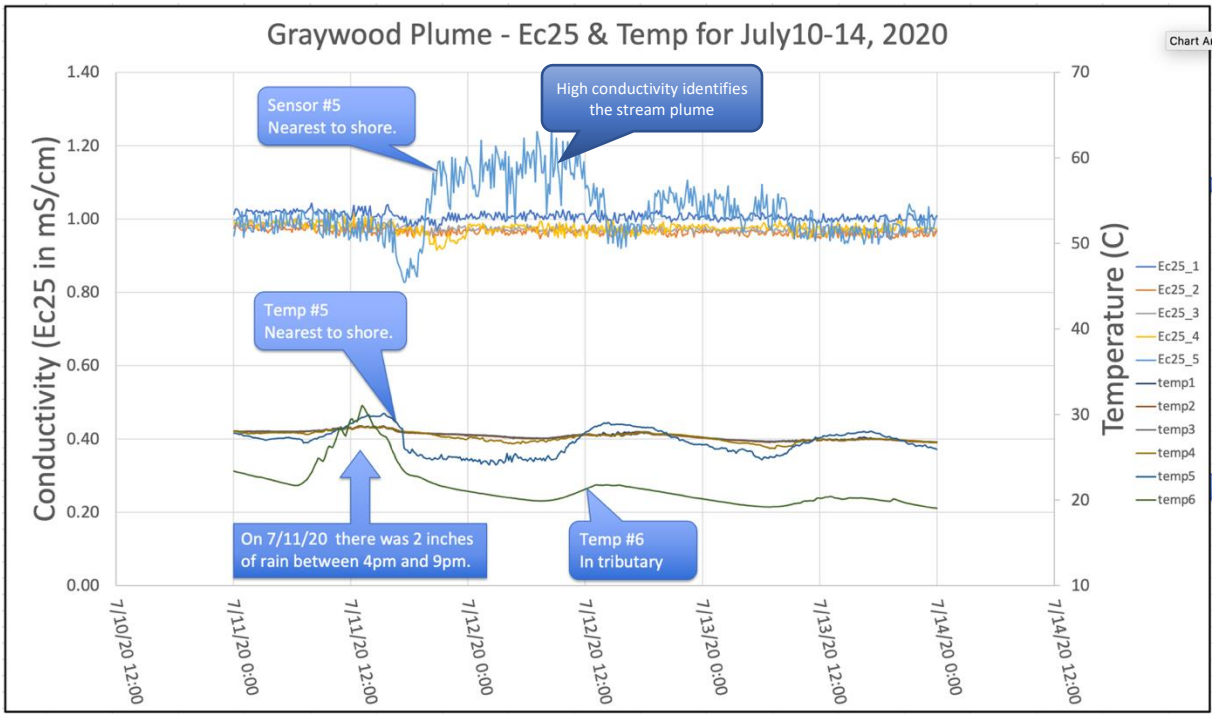

The system recorded a significant change of conductivity for sensor number 6 which is located approximately 8 meters from the mouth of the tributary but did not record a significant change for the other 4 sensors located more than 55 meters from the tributary. This result implies that conductivity is not an appropriate parameter for use in tracking plume distribution for tributary nutrients. It is possible that more sensitive sensors might be able to improve the results but given the limited change in conductivity observed, it seems unlikely.

In addition to the conductivity sensors, as conditions permitted, a drone was used to capture images of visible material that was brought into the lake by a tributary. The drone was used in several locations over the lake immediately following heavy downpours. The resulting images showed the influx of expansive plumes that undoubtedly bring large quantities of silt and nutrients into the lake. These introduced nutrients are referred to as “external loading.” (Nutrients that are already in the lake and get redistributed are referred to as “internal loading.”) While recent studies show that “internal loading” is the dominant source of nutrients coming into the ecosystem of Conesus Lake, external loading is also significant especially in providing nutrients that fuel the growth of nearshore filamentous algae and macrophyte beds. It is also worth noting that external loading this year provides material that can be a part of internal loading in future years.

The use of drones is limited to rain events that have periods of clear weather immediately following periods heavy rain at times and in locations that a drone operator is available. The photos below give you an idea just how extensive these sediment plumes can be.

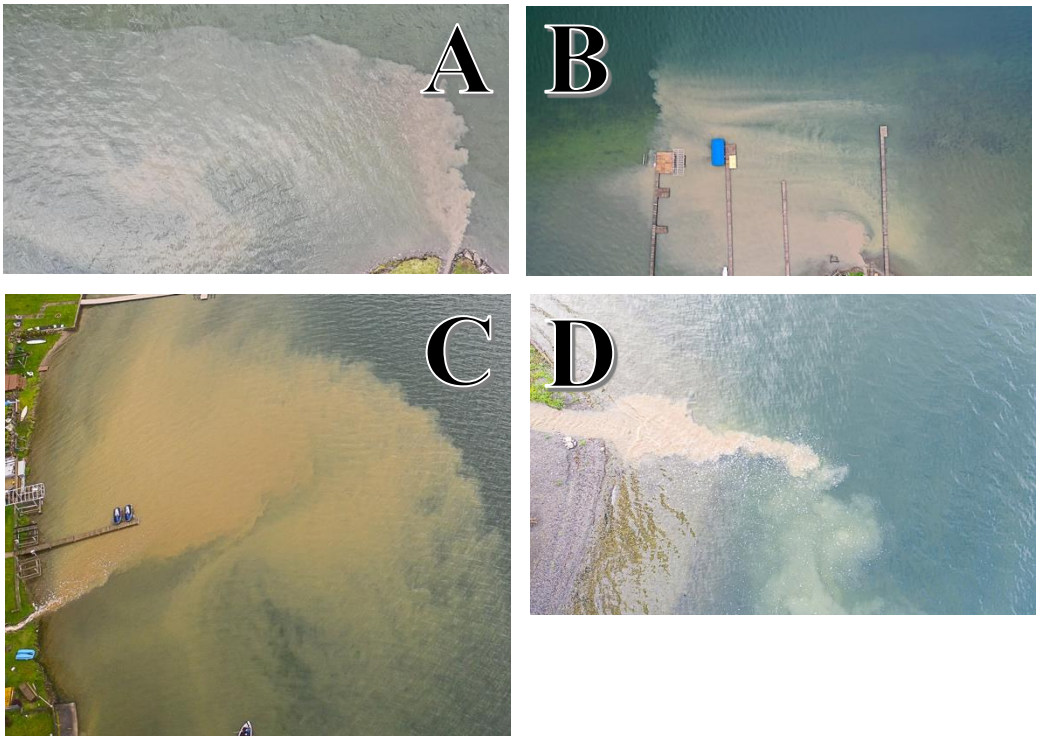

From observation, there seem to be a few types of tributary plumes:

- Recurring plumes – These are plumes that appear regularly following significant rainfall. Perhaps they are related to continuous erosion along the tributary route. Most of the plume producing tributaries seem to recur following significant rain events.
- Sporadic plumes – These are plumes that seem to appear sometimes; not every rainfall triggers this kind of plume. These may be related to a one-time onshore activity or they might follow a kind of “spring-cleaning” event. (Photo “C” is an example of this)
- Plumes that “fan-out” across the surrounding shallows. The sediment is generally left above the thermocline layer in the summer where plants can take advantage of the added nutrients. This seems to be the typical situation. (Photos “A”, “B” and “C”)
- Plumes that seem to go directly into the deep water without much sediment left in the shallow area. These are associated with deep water being very near the shore and are less common. The sediments appear to descend below the thermocline, it is unclear how deep the sediments go (Photo “D”). It is possible that this type of plume affects our estimate of internal loading by introducing

nutrients below the thermocline where the dominant nutrient source for internal loading is located.

So far, no significant effort has been made to identify the source(s) of the sediment. It seems likely that a combination of erosion and development activities are responsible for the widespread occurrence of these sediment plumes. It is also important to remember that the source(s) can be virtually anywhere in the watershed.

Future efforts to evaluate might use turbidity sensors that measure light transmission and scattering to detect the presence of particles in the water. Continued surveillance using drones or other aerial platforms might also provide insight on the distribution of sediments.

Appendix II. Report on Late Season Phytoplankton Bloom

Characterization of Late Season Phytoplankton Bloom

Brooke Drexler, Katheryne Hibbert-Nelson,
Sarah Metz and Isidro Bosch

ABSTRACT

This study examined the phytoplankton community of Conesus Lake in September and October 2020 to determine if this unusual trend of limited cyanobacterial representation in summer continued into the fall bloom. Phytoplankton samples were taken on September 17th and October 14th by vertical net haul, concentrated and preserved in 40% final concentration of Ethanol for later analysis of species dominance. Biomass metrics of water transparency and chlorophyll a biomass showed that the September community was in the midst of a moderate bloom dominated by the diatoms *Fragilaria*, *Melosira*, and the cyanobacterium *Lyngbya*. By October, the bloom had progressed in intensity, as indicated by higher chlorophyll a and lower water clarity, and a shift in the dominant species occurred to *Melosira*, *Asterionella,* and the green alga *Meogotia*. We concluded that 2020 was an unusual year, as the late season bloom was dominated by diatoms, not cyanobacteria. Lower temperatures and wind driven water column mixing events that occurred in September and mid-October may account for the differences from previous years.

INTRODUCTION

Phytoplankton blooms in Conesus Lake in recent years have followed a seasonal pattern in which late summer and early fall communities are typically dominated by cyanobacteria. The dominant species are cyanobacteria in the genera *Dolichospermum*, *Lyngbya*, *Oscillatoria* and *Woronichinia* while *Microcystis*-dominated blooms occur infrequently. Cyanobacteria have the ability to out-compete other phytoplankton when temperatures are high because they are more efficient at absorbing dissolved nutrients. This is an advantage during periods of nutrient limitation that are typical of temperate lakes in late summer, prior to turnover. Late summer and fall are times when cyanobacterial blooms occur and colonies may accumulate nearshore in concentrations that pose a potential health hazard (i.e., Harmful Algal Blooms). Cyanobacteria have the ability to release toxins that can be harmful, causing skin irritation and illness if swallowed (Blue Green Algae, Livingston County). Harmful algal blooms can lead to decreased water clarity and loss of lake ecosystem services, such as recreational use, property value and water supply safety. Known contributors to cyanobacterial blooms can vary. Nutrient runoff, warmer than usual temperatures and water column mixing events are some possible causes (Bosch et al., 2015).

In the summer of 2020, Conesus Lake did not follow the typical patterns seen in previous years. Only one harmful algal bloom was recorded in June (Personal Communication, Livingston County Department of Health). This was unusual because in a typical year in Conesus Lake can experience blooms dominated by species of *Dolichospermum* beginning in July that last well into August. The blooms may wane in Early August but re-emerge in late summer when mixing of phosphorus from the hypolimnion ensues.

Although less abundant in Conesus Lake, *Microcystis* is also able to cause toxic blooms in freshwater communities (Ohtake et al., 1989). These phytoplankton are important to study. Microcystis-dominated blooms in Lake Erie serve as a harbinger for other lakes, and emphasize the importance of management plans to control phytoplankton blooms (Michalak et al., 2013). With climate warming on the rise, lakes may be more prone to experience harmful algal blooms.

Building on the observations of reduced cyanobacterial abundance during summer 2020, we hypothesized that this trend would continue into the fall bloom period typical of Conesus Lake and other temperate lakes. Specifically, the goal of this study was to document the composition of the phytoplankton community during the late season to determine if the summer trend of limited cyanobacteria representation would continue, or if there would be a return of cyanobacterial dominance that is more typical of Conesus Lake. To do this, we characterized the two phases of the fall bloom by collecting data from September 17th and October 14th.

METHODS

Water samples were collected on September 17th and October 14th 2020 from the south basin of Conesus Lake over a depth of 18m. Water column profiles were collected using a Hydrolab 4A multiparameter sonde. These parameters included temperature (°C), depth (m), photosynthetically active radiation (in µEinsteins. m^{-2} .sec^{-1} of 400-700 nm wavelengths), conductivity (µSiemens.cm^{-2}), dissolved oxygen (mg.L^{-1} and % saturation) and redox potential (mV). Sensors were calibrated prior to deployment in accordance with the manufacturer's specification and using purchased Hach standards for turbidity, conductivity, ORP and pH. Only the light profile data was used for the purpose of this study.

Water clarity was documented using three different parameters. Water turbidity was measured for each sample using a calibrated Hach 2100P turbidity meter in units of nephelometer turbidity units (NTU). The Secchi Depth was determined for each sample using a 20-cm black and white Secchi disc. Lastly, the light attenuation coefficient was calculated from profile data on both dates using the following relationship: $I_z = I_0 * e^{-n}$. This relationship is solved for n:

$$n = (\ln(I_z)) - \ln(I_0)) / I_0 \text{ depth} - \text{depth } I_z$$

For chlorophyll a analysis we followed procedures in Standard Methods for the Analysis of Water and Wastewater Analyses of water samples (USEPA, 1999). Water samples were collected from 0.5 and 3 m below the surface using a 2.2 L van Dorn

water sampler. The water samples were placed in acid-washed plastic bottles and held in ice for transport. Prior to collection, each of the sample containers were rinsed with the water being collected. Within 4 hours of collection, a known volume of each sample was filtered through a GFF fiber filter. Filters were folded and individually placed in aluminum foil and stored at -20 ℃ in a freezer until analysis in November. Filters were broken up as much as possible and extracted with 15 mL of 90% alkalized acetone for about 10-12 hours. After this time, the filters were once again ground down to smaller fragments and extraction was allowed to continue for another 6-8 hours. After the extraction period, the samples were spun in a desktop centrifuge at 1000 rpm for 3 minutes. The supernatant was removed with a 9’ glass pipette, being careful not to pick up remaining filter material. The samples were analyzed fluorometrically using a desktop Turner Fluorometer.

Vertical net samples were used to study the relative abundance of phytoplankton species during the two dates. A 0.5 m plankton net with 163 micron mesh size was allowed to sink mouth first to about 10 m and then hauled vertically through the water column. Samples were preserved in 40% ethanol. We observed the net samples for both dates under a microscope at 100x total magnification to distinguish different phytoplankton species. Relative abundance for each species was estimated using colony/individual counts. Species were determined using the phytoplankton key provided (Baker et al., 2012).

To measure the productivity of Conesus Lake, we calculated TSI values to further compare the two bloom periods. Using Secchi depth and chlorophyll a values, we calculated TSI values for each parameter and took the average value to determine the productivity. The formulas used to solve for TSI:

$$TSI\ (SD) = 60 - 14.1 * \ln(SD)$$

$$TSI\ (chl\ a) = 9.81 * \ln(chl\ a) + 30.6$$

RESULTS

Indicators of phytoplankton biomass in the south basin of Conesus Lake including chlorophyll a concentration, Secchi depth, light attenuation coefficients and turbidity are reported in **Table 1** for September 17th, 2020 and October 14th, 2020. The average chlorophyll a concentration was 13.2 mg/L for September 17th, 2020 and 32.6% higher with 17.5 mg/L for October 14th, 2020. Similarly, the secchi depth on September 17th was recorded as 3.1 m. whereas on October 14th, the secchi depth was 1.8 m. This indicates that the water clarity was lower on October 14th than on September 17th and is consistent with our observation that the water during the October collection date was somewhat brown and turbid. The light attenuation coefficient was 0.509 $\pm$ 0.071 for September 17th and 0.93 $\pm$ 0.11 for October 14th. Turbidity was only slightly higher at 2.1 NTU on October 14th than in September 17th (1.9 NTU) but the differences are consistent in phytoplankton biomass and other measurements in **Table 1**.

The Carlson's Trophic State Index was calculated for both bloom periods of Conesus Lake: September 17th and October 14th. For September 17th, the TSI was 48.8 according to chlorophyll a and 51.9 according to Secchi depth, resulting in an average TSI of 50.4. For October 14th, TSI was 51.6 according to chlorophyll a and 51.7 according to Secchi depth, resulting in an average TSI of 51.6 and indicates a higher productivity.

Microscopic analysis indicates that diatoms were dominant in both net samples analyzed (**Table 2, Figures 3 and 5**). We did not attempt to identify samples to species, so only genera are reported for most groups. On September 17th species of *Fragilaria* had the highest relative abundance with 59%, followed by *Melosira* with 16%, and finally *Lyngbya* with 7% (**Fig. 2)**. Cyanobacteria were prominent and represented primarily by the large filaments of *Lyngbya* and a few colonies of *Microcystis*. By October 14th, the dominant diatoms were *Melosira* with a relative abundance of 52% and *Asterionella* at 7%, while *Fragilaria* was much less abundant at 5%. The green alga that we identified as *Mougeotia* was second in abundance at 33% with its very small filaments (**Table 3**). Cyanobacteria were present but poorly represented in the October sample with a relative abundance of 1% *Dolichospermum* and less than 1% *Lyngbya*.

DISCUSSION

According to all of the metrics reported including Secchi depth, turbidity, light attenuation coefficient and chlorophyll a analysis, it appears that we sampled the start of a bloom on September 17th that had proliferated into a significant bloom by mid-October when we noted the water was very brown and there was especially low water clarity and high chlorophyll a concentration. In the September collection, the dominant phytoplankton were *Fragilaria*, *Melosira*, and *Lyngbya*. October showed dominance of *Melosira, Meogotia*, and *Asterionella*. Although the bloom was not a harmful algal bloom, the lake still remained productive. The TSI calculated indicates there was little change in TSI value between the two bloom periods, September 17th and October 14th, but October 14th proved to be slightly more productive. Reported by Makarewicz and Lewis in 2014, the long term average of Conesus Lake was a TSI of 49.3, which is not far off from what we found in 2020 (Makarewicz, 2014). The trophic state of the fall bloom remained fairly stable, even though the dominant phytoplankton have changed from September 17th to October 14th.

This late season growth period was dominated by diatoms from the genera *Fragilaria*, *Melosira* and *Asterionella*. This proved to be different from previous years, when cyanobacteria blooms dominated the fall season and caused a number of harmful algal blooms around the lake. Cyanobacterial blooms in Conesus Lake are typically dominated by *Dolichospermum*, though other species including types of *Microcystis* also flourish (Bosch et al., 2018). Summer cyanobacterial blooms are also typical of Conesus Lake (Bosch et al., 2015), but 2020 was unusual in having only one major cyanobacteria dominated bloom reported in June. This was a moderate bloom dominated by *Dolichospermum* (Personal Communication, Livingston County Department of Health). Very little *Dolichospermum* were observed during the 2020 late season (September and October), and there were no harmful algal blooms reported. Some colonies were recorded from the October 14th sample, but they were a tiny fraction of the phytoplankton biomass. *Lyngbya*, was 7% of the colonies/cells on September 17th. This genus of cyanobacteria is known to produce toxins and form “slicks” on the surface of lakes. However, there were no “slicks” reported for Conesus Lake during the summer and we certainly did not see surface accumulations during the

late season sampling period in 2020. In conclusion, the fall bloom was consistent with the summer months, as there was little cyanobacteria present.

The dominance of diatoms in the late season sharply contrasts previous years when cyanobacteria made up the bulk of the biomass and at times caused harmful algal blooms (Bosch et al., 2015). We speculate that this unusual trend in 2020 may be related to wind-driven water column mixing events that delivered nutrients and colder waters to the surface. Moreover, water temperature in September of 2020 was lower than average, as we discuss below. These conditions may have favored diatom growth instead of the more typical proliferation of cyanobacteria. Temperature arrays deployed in the lake indicate that there were major water column mixing events prior to both water collection dates, caused by strong winds on September 7th, September 12th, October 12th and October 13th (**Fig. 6**). During these mixing events, nutrients and cold water typically are delivered from the hypolimnion to the upper lake layers. This influx of nutrients and cold water may have been the reason that cyanobacteria were less abundant. Cyanobacterial growth can thrive when temperatures are warmer and there are low concentrations of nutrients available. This is due to the higher SA/V of their small cells compared to that of larger phytoplankton, which are less efficient at absorbing nutrients. With delivery of phosphorus from the hypolimnion, the competitive balance may have shifted to the diatoms. This assumes that there was also an ample supply of nitrogen in the water. That nitrogen may have been provided during the early stages of the blooms by the dominant *Lyngbya*, which is recognized to be a diazotroph (an aerobic nitrogen fixer). Additionally, the cold water coming from the bottom of the lake can cool the surface temperature and can allow diatoms to take over.

Harmful algal blooms are often linked to warmer temperatures. Diatoms as mentioned above, are more successful in cooler waters. We obtained data on surface water temperatures in the lake from the Avon Water plant, which has an intake that draws from a depth of about 7 m that is still within the epilimnion. According to the long term record of the water plant, September 2020 was about a half a degree colder than normal (**Fig. 7**), which may have been beneficial for diatom growth. Mixing events and lower surface temperatures are two factors that may have contributed to the unusual patterns of phytoplankton biomass we observed in September and October 2020.

REFERENCES

Baker, A.L. et al. 2012. Phycokey -- an image based key to Algae (PS Protista), Cyanobacteria, and other aquatic objects. University of New Hampshire Center for Freshwater Biology. http://cfb.unh.edu/phycokey/phycokey.htm 18 Dec 2020. “Blue Green Algae.” *County Seal*, www.livingstoncounty.us/785/Blue-Green-Algae.

Bosch, I., Chislock, M., Warner, K., Bell, E., Hanafin, K., “Monitoring of Internal Phosphorus Loading, Water Column Mixing, Cyanobacterial Blooms and Dreissenid Mussels in Conesus Lake NY (Summer 2018)”, 15 February 2019.

Bosch, I., Connors, D., McCabe, C., Wong, G., Bowling, A., Kublik, A., “Linkage Between Water Column Mixing of Phosphorus and Onset of Cyanobacteria Blooms in Conesus Lake, (NY)”, 1 December 2015.

CSLAP Report Search. 9 Jan. 2019, nysfola.org/cslap-report-search/. Department of Environmental Conservation, et al. “Harmful Algal Bloom Action Plan Conesus Lake.” *Department of Environmental Conservation*, www.dec.ny.gov.

Makarewicz, Joseph C. and Lewis, Theodore W., "Trophic Status of Conesus Lake 2014: Long-term Trends in Lake Chemistry and the Plankton Community" (2014). *Technical Reports*. 130. https://digitalcommons.brockport.edu/tech_rep/130.

Michalak, A. M., et al. “Record-Setting Algal Bloom in Lake Erie Caused by Agricultural and Meteorological Trends Consistent with Expected Future Conditions.” *Proceedings of the National Academy of Sciences*, vol. 110, no. 16, 2013, pp. 6448–6452., doi:10.1073/pnas.1216006110.

Ohtake, A, et al. “Toxicity of Microcystis Species Isolated from Natural Blooms and Purification of the Toxin.” *Applied and Environmental Microbiology*, vol. 55, no. 12, 1989, pp. 3202–3207., doi:10.1128/aem.55.12.3202-3207.1989.

USEPA. 1999. *Methods for the Chemical Analysis of Water and Wastes*. Environmental Monitoring and Support Laboratory. Environmental Protection Agency. Cincinnati, Ohio. EPA-600/4-79-020.

TABLES/FIGURES

Table 1. Turbidity, Secchi depth, Average Attenuation Coefficient, and acetone extracted chlorophyll a concentration for the South Basin of Conesus Lake for September 17th, 2020 and October 14th, 2020.

Location	Date	Depth (m)	Turbidity (NTU)	Secchi Depth (m)	Average Attenuation Coefficient (2 -7m)	Chlorophyll a Concentration (mg/L)
South Basin of Conesus Lake	17-Sep	0 - 3	1.9	3.1	0.509 +/- 0.071	0.5 m: 13.71 3.0 m: 12.65
South Basin of Conesus Lake	14-Oct	0 - 3	2.1	1.8	0.930 +/-0.11	0.5 m: 17.47 3.0 m: 17.60 6.0 m: 16.05

Table 2. Colony/ individual counts and % composition of phytoplankton from vertical net haul taken in the South Basin of Conesus Lake on September 17th, 2020.

September 17th		
Identification	**Colony/Individual Counts**	**% of total**
Diatoms		
Fragilaria sp.	92	59
Melosira sp.	25	16
Asterionella sp.	1	1
Synedra sp.	1	1
Stephanodiscus sp.	1	1
Cyanobacteria		
Lyngbya sp.	11	7
Microcystis sp.	9	6
Merismopoedia sp.	1	1
Dinoflagellates		
Ceratium sp.	3	2
Golden Brown Algae		
Dinobryan sp.	7	4
Green Algae		
Pediastrium sp.	4	2
Total colonies/individuals	155	

Table 3. Colony/ individual counts and % composition of phytoplankton from vertical net haul taken in the South Basin of Conesus Lake for October 14th, 2020.

October 14th		
Identification	**Colony/Individual Counts**	**% of total**
Diatoms		
Melosira sp.	128	52
Asterionella sp.	16	7
Fragilaria sp.	13	5
Cyanobacteria		
Dolichospermum sp.	2	1
Lyngbya sp.	1	<1%
Dinoflagellates		
Dinobryan sertularia	6	2
Green algae		
Mougeotia sp.	81	33
Total colonies/individuals	247	

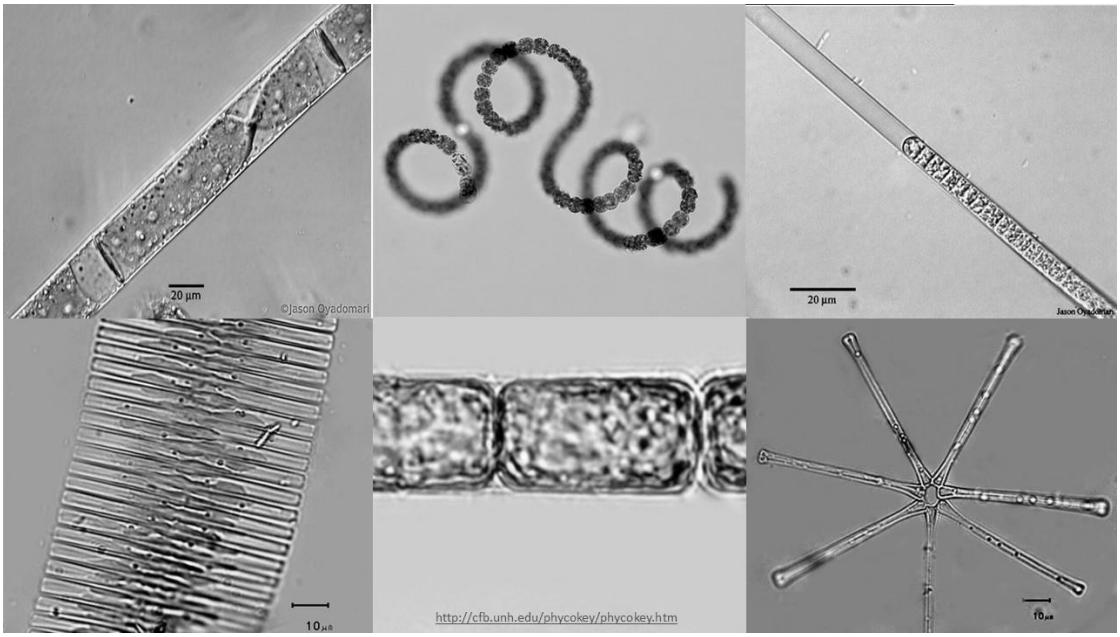

Figure 1: Three dominant phytoplankton species were identified from each date by microscopic analysis. On September 17th, the dominant species were *Melosira* (bottom center), *Lyngbya* (top right) and *Fragilaria* (bottom left). On October 14th the dominant species were *Mougeotia* (top left), *Asterionella* (bottom right) and *Dolichospermum* (top center) (Images from Baker et al., 2012).

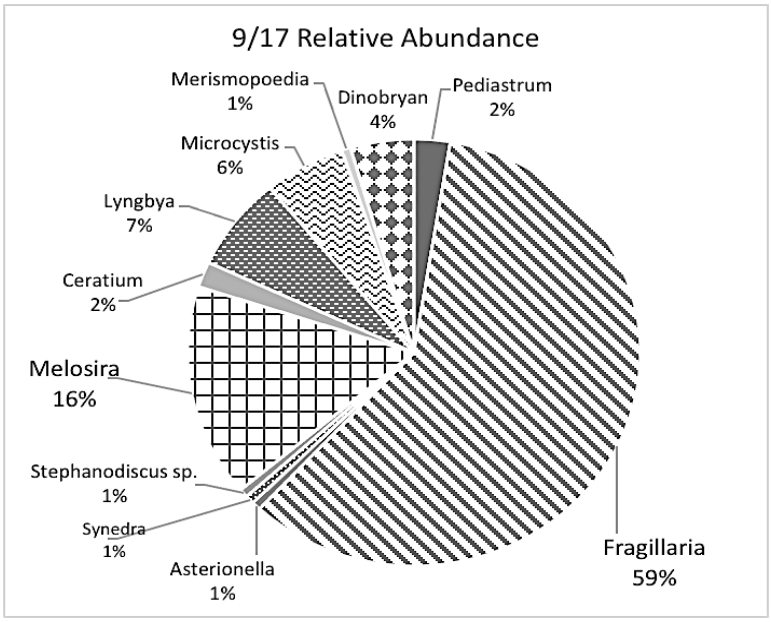

Figure 2. Relative abundance of phytoplankton by genera for the South Basin of Conesus Lake on September 17th.

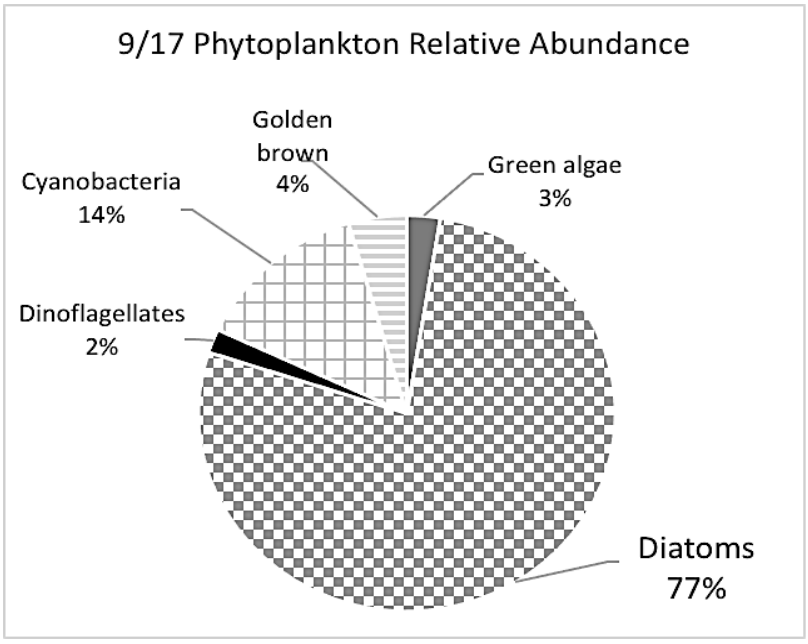

Figure 3 . Relative abundance of major phytoplankton taxonomic groups for the South Basin of Conesus Lake on September 17th.

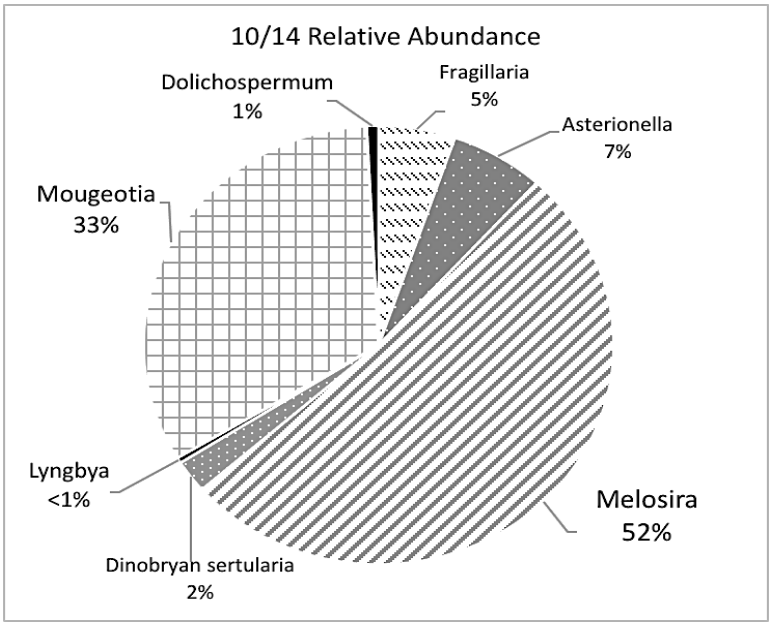

Figure 4. Relative abundance of phytoplankton by genera for the South Basin of Conesus Lake on October 14th.

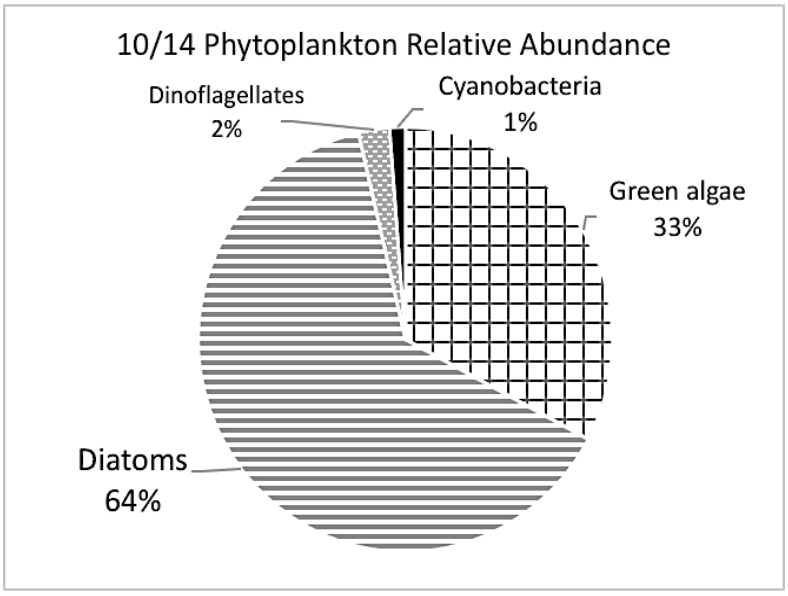

Figure 5. Relative abundance of major phytoplankton taxonomic groups for the South Basin of Conesus Lake on October 14th.

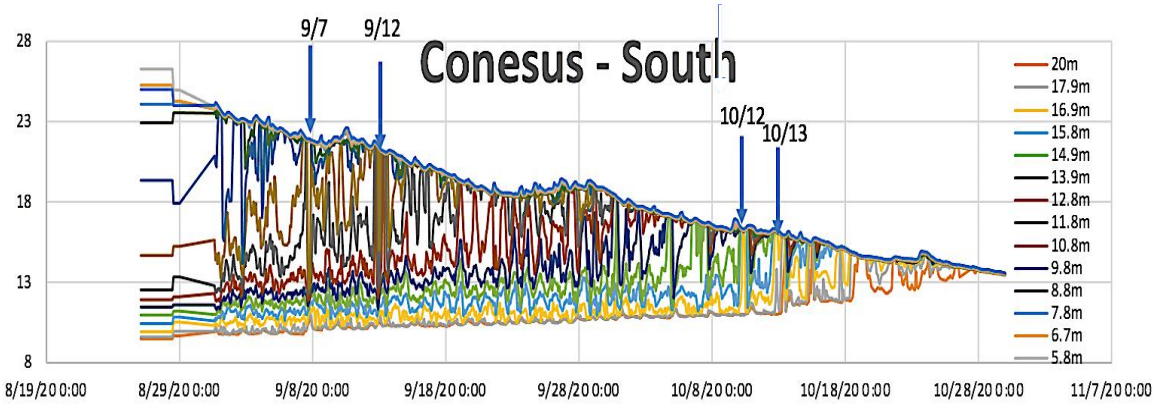

Figure 6. Temperature data from *in situ* temperature array shows major mixing events taking place (where bottom temperatures approach surface temperatures) in September and October, which are identified on the graph. (Arrays are courtesy of Livingston County Planning Department.)

Appendix III. Macrophyte quadrat biomass data as blotted dry weight.

Sand Point Gully					
18-Jun-20	Total	Wet Weight	Wet Wt.	Wet Wt.	Wet Wt.
Sand Point	Wet Wt (g)	watermilfoil	Coontail	Eelgrass	Sago
North Transect					
3 m	157.9	157.9			
3	306	306			
3	225.4	225.4			
2 m	201.3	201.3			
2	420.8	420.8			
2	271.6	271.6			
1 m	117.4	114.9			2.5
1	68.6	68.6			
1	209.8	209.7			0.1
18-Jun-20	Total	Wet Wt	Wet Wt.	Wet Wt.	Wet Wt.
Sand Point Gully	Wet Wt (g)	watermilfoil		Eelgrass	Sago
Center Transect					
3 m	50.8	50.8			
3	305.1	305.1			
3	310.8	310.8			
2m	105.5	105.5			
2	146.6	146.6			
2	497.2	497.2			
1 m	121.2	120.2		0.8	0.2
1	143.8	143.8			
1	68.1	68.1			
18-Jun-20	Total	Wet wt.	Wet wt.	Wet wt.	Wet wt.
Sand Point Gully	wet wt (g)	watermilfoil		Eelgrass	Sago
South Transect					
3 m	193	193			
3	296	296			
3	173	173			
2 m	143.2	143.2			
2	141	140.6		0.4	
2	135.2	134.5		0.7	
1 m	40.3	27.1		13.2	
1	179.1	140.8		31	7.3
1	159	150.1		8.6	0.3

Appendix III. Continued (Sand Point Gully)

14-Jul-20	Total	Wet wt.	Wet wt.	Wet wt.	Wet wt.
Sand Point Gully	Wet Wt. (g)	watermilfoil	Coontail	Eelgrass	
North Transect					
3 m	260.4	260.4			
3	239.9	239.9			
3	88.7	75.5	13.2		
2 m	234.5	234.5			
2	174.8	174.8			
2	177.7	177.7			
1 m	177.7	177.7			
1	476	253.5		222.5	
1	114.4	114.4			
14-Jul-20	Total	Wet wt.	Wet wt.	Wet wt.	Wet wt.
Sand Point	Wet Wt. (g)	Watermilfoil	Coontail	Eelgrass	
Center Transect					
3 m	195.3	195.3			
3	119.7	119.7			
3	65.9	65.9			
2m	278.5	278.5			
2	175.9	155	20.9		
2	180.5	152		28.5	
1 m	183.3	132.4		50.9	
1	83.1	43.4		39.7	
1	78.1	78.1			

14-Jul-20	Total	Wet wt.	Wet wt.	Wet wt.	Wet wt.
Sand Point	Wet Wt. (g)	Watermilfoil	Coontail	Eelgrass	Sago
South Transect					
3 m	194.5	194.5			
3	237.7	237.7			
3	106.1	106.1			
2 m	146.38	103.5		42.88	
2	264.4	200.5		63.9	
2	119.82	54.9		64.92	
1 m	182.7	162.6		20.1	
1	327	327			

Appendix III. Continued (Sand Point Gully)

13-Aug-20	Total	Wet wt.	Wet wt.	Wet wt.	Wet wt.
Sand Point	Wet Wt. (g)	Watermilfoil	Coontail	Eelgrass	Sago
North Transect					
3 m	193	193			
3	296	296			
3	173	173			
2 m	143.2	143.2			
2	141	140.6		0.4	
2	135.2	134.5		0.7	
1 m	40.3	27.1		13.2	
1	179.1	140.8		31	7.3
1	159	150.1		8.6	0.3
13-Aug-20	Total	Wet wt.	Wet wt.	Wet wt.	Wet wt.
Sand Point	Wet Wt (g)	Watermilfoil	Coontail	Eelgrass	
Center Transect					
3 m	257	257			
3	327	327			
3	270.8	270.8			
2m	387.7	387.7			
2	327.7	301		26.7	
2	292.6	283.3		9.3	
1 m	0	no plants			
1	0	no plants			
1	0	no plants			
13-Aug-20	Total	Wet wt.	Wet wt.	Wet wt.	Wet wt.
Sand Point	Wet Wt (g)	Watermilfoil	coontail	Eelgrass	
South Transect					
3 m	224.5	224.5			
3	186.8	186.8			
3	170.6	170.6			
2 m	244.4	244.4			
2	369.4	250.0		119.4	
2	0				
1 m	0				
1	0				
1	0				

Appendix III. Continued (North Gully)

North Gully					
22-Jun-20	Total	Wet wt.	Wet Wt.	Wet Wt.	Wet Wt.
North Transect	Wet Wt (g)	Watermilfoil	Coontail	Eelgrass	Sago
3 m	8.2	2.2		6	
3	46.7	45.5		1.2	
3	32.8	27.4		5.4	
2 m	79.1	74.8		4.3	
2	107.5	105		2.5	
2	108.4	108.2		0.2	
1 m	105.3	102.9			2.4
1	187.9	183.5		0.1	4.3
1	242.8	133.2		0.2	
22-Jun-20	Total	Wet Wt.	Wet Wt.	Wet Wt.	Wet Wt.
Center Transect	Wet Wt (g)	Watermilfoil	Coontail	Eelgrass	
3 m	38.8	38.8			
3	31.4	31.4			
3	71.8	71.8			
2m	74	74			
2	144.1	144.1			
2	117.9	117.9			
1 m	274.5	273.9		0.6	
1	100	99.2		0.8	
1	100.3	100.3			
22-Jun-20	Total	Wet Wt.	Wet Wt.	Wet wt.	Wet wt.
South Transect	Wet Wt (g)	Watermilfoil	Coontail		
3 m	69.6	69.6			
3	60.2	60.2			
3	41.9	41.9			
2 m	84.4	84.4			
2	96.5	96.5			
2	242.8	242.8			
1 m	9.8	9.8			
1	87.4	87.4			
1	82.1	82.1			

Appendix III. Continued (North Gully)

North Gully					
15-Jul-20	Total	Wet Wt.	Wet Wt.	Wet Wt.	Wet Wt.
North Transect	Wet Wt (g)	Watermilfoil		Eelgrass	
3 m	171.2	171.2			
3	159.2	159.2			
3	134.6	134.6			
2 m	377.7	377.7			
2	358.3	358.3			
2	236	236			
1 m	No milfoil				
Center Transect	Total	Wet Wt.	Wet Wt.	Wet Wt.	Wet Wt.
15-Jul-20	Wet Wt (g)	Watermilfoil		Eelgrass	
3 m	329.9	329.9			
3	244.1	244.1			
3	229.8	229.8			
2m	444	444			
2	291	291			
2	352.1	352.1			
1 m	no milfoil				
South Transect	Total	Wet wt.	Wet Wt.	Wet Wt.	Wet Wt.
15-Jul-20	Wet Wt. (g)	Watermilfoil		Eelgrass	
3 m	243	243			
3	382.6	382.6			
3	229.3	229.3			
2 m	559.1	559.1			
2	410.8	410.8			
2	480.2	480.2			
1 m	no milfoil				

Appendix III. Continued (North Gully)

North Gully					
10-Aug-20	Total	Wet Wt.	Wet Wt.	Wet Wt.	Wet Wt.
North transect	Wet Wt (g)	Watermilfoil		Eelgrass	
3 m	171.2	171.2			
3	159.2	159.2			
3	134.6	134.6			
2 m	377.7	377.7			
2	358.3	358.3			
2	236	236			
1 m	No milfoil				
1					
Center Transect	Total	Wet Wt.	Wet Wt.	Wet Wt.	Wet Wt.
10-Aug-20	Wet Wt (g)	Watermilfoil		Eelgrass	
3 m	329.9	329.9			
3	244.1	244.1			
3	229.8	229.8			
2m	444	444			
2	291	291			
2	352.1	352.1			
1 m	no milfoil				
South Transect	Total	Wet Wt.	Wet Wt.	Wet Wt.	Wet Wt.
10-Aug-20	Wet Wt (g)	Watermilfoil		Eelgrass	
3 m	243	243			
3	382.6	382.6			
3	229.3	229.3			
2 m	559.1	559.1			
2	410.8	410.8			
2	480.2	480.2			
1 m	no milfoil				

Appendix III. Continued (Cottonwood Gully)

Cottonwood Gully					
25-Jun-20	Wet Wt. (g)	Wet Wt.	Wet Wt.	Wet Wt.	Wet Wt.
Cottonwood North	Total	Watermilfoil		Eelgrass	
3 m	No Plants				
3	No Plants				
3	No Plants				
2 m	128.3	128.3			
2	161.2	161.2			
2	155.3	155.3			
1m	7.4			7.4	
1	133.4	116.9		16.5	
1	25.1	13.4		11.7	
Cottonwood Gully					
13-Jul-20	Wet Wt. (g)	Wet Wt.	Wet Wt.	Wet Wt.	Wet Wt.
Cottonwood North	Total	milfoil		Eelgrass	
3 m	No Plants				
3	No Plants				
3	No Plants				
2 m	236.5	236.5			
2	111.3	111.3			
2	71.6	71.6			
1 m	No Plants				
1	No Plants				
Cottonwood Gully					
10-Aug-20	Wet Wt. (g)	Wet Wt.	Wet Wt.	Wet Wt.	Wet Wt.
Cottonwood North	Total	milfoil		Eelgrass	
3 m	No Plants				
3	No Plants				
3	No Plants				
2 m	185.6	177.5		8.1	
2	218.4	218.4			
2	132.7	132.7			
2	157.6	157.6			
2	195.8	195.8			
1 m	No Plants				
1	No Plants				

Appendix III. Continued (Graywood Gully)

Graywood Gully	Wet Wt (g)	Wet Wt.	Wet Wt .	Wet Wt.	Wet Wt.
25-Jun-20	Total	WaterMilfoil	Coontail	Eelgrass	Stargrass
Graywood South					
3m	73.7	73.7			
3	92.9	92.9			
3	76.2	76.2			
2m	50.7	50.5		0.2	
2	185.8	182.6	3.2		
2	69.4	66.9		2.5	
1m	No Plants				
1	No Plants				
1	No Plants				
Graywood Center	Wet Wt (g)	Wet Wt.	Wet Wt .	Wet Wt.	Wet Wt.
	Total	Watermilfoil	Coontail	Eelgrass	Stargrass
3 m	10.2		7.2	3	
3	23.9			23.9	
3	25.7	4			
2 m	97.7	97.7			
2	96.9	96.9			
2	28	27.1			0.9
1	67.1	67.1			
1 m	27.5	27.5			
1	74.1	74.1			
Graywood North	No Plants				

Appendix III. Continued (Graywood Gully)

Graywood Gully					
15-Jul-20	Wet Wt (g)	Wet Wt.	Wet Wt .	Wet Wt.	Wet Wt.
Graywood South	Total	Watermilfoil	Coontail	Eelgrass	Stargrass
3 m	139.8	87.9	51.9		
3	132.4	122.1	10.3		
3	152	128.3	23.7		
2 m	49.3	43.6		5.7	
2	29.7	22.6		7.1	
2	58.9	52.6	4.1	2.2	
2.5 m	203.9	172.3	31.6		
1	no milfoil				
1	no milfoil				
1	no milfoil				
Graywood Center	Wet Wt (g)	Wet Wt.	Wet Wt .	Wet Wt.	Wet Wt.
	Total	Watermilfoil	Coontail	Eelgrass	Stargrass
3 m	74.7	74.7			
3	155.2	155.2			
3	107.1	105.6		1.5	
2m	73.2	63.7		9.5	
2	59.2	59.2			
2	87.4	83.4		4	
1 m	no milfoil				
1	no milfoil				
1	no milfoil				
Graywood North	Wet Wt (g)	Wet Wt.	Wet Wt .	Wet Wt.	Wet Wt.
	Total	Watermilfoil	Coontail	Eelgrass	Stargrass
3	60.5	51.6		8.9	
3	60	28.7		31.3	
3	164	131.3		32.7	
2	35.7	24.7		11	
2	69.7	0.9		68.8	
2	171.2	144.9		26.3	
1	no milfoil				
1	no milfoil				

Appendix III. Continued (Graywood Gully)

Graywood Gully					
26-Aug-20	Wet Wt (g)	Wet Wt.	Wet Wt.	Wet Wt.	Wet Wt.
Graywood South	Total	Watermilfoil	Coontail	Eelgrass	Stargrass
3 m	466.8	188.1	278.7		
3	127.5	127.5	0		
3	278	277.8	0.2		
2	584	112	472		
2	491.9	424	67.9		
2	592.6	437.7	154.9		
1 m	No milfoil				
Graywood Center	Wet Wt (g)	Wet Wt.	Wet Wt.	Wet Wt.	Wet Wt.
	Total	Watermilfoil	Coontail	Eelgrass	Stargrass
3 m	236.2	208	28.2		
3	638.7	481.9	156.8		
3	305.7	280.4	25.3		
2 m	712.8	525.5	187.3		
1m	No milfoil				
Graywood North	Wet Wt (g)	Wet Wt.	Wet Wt.	Wet Wt.	Wet Wt.
	Total	Watermilfoil	Coontail	Eelgrass	Stargrass
3m	60.5	51.6		8.9	
3	60	28.7		31.3	
3	164	131.3		32.7	
2m	35.7	24.7		11	
2	69.7	0.9		68.8	
2	171.2	144.9		26.3	
1	no milfoil				

Appendix IV. Results of September North Basin Survey. Data are reported as blotted dry weight and dry weight converted. The latter is calculated from blotted dry weight/ oven dried weight ratios*.

Site	Species #	Species	Blotted Dry Weight (g)	*Final DW (g)	*Total DW Per site (g)
Old Orchard Cove	1.	Coontail	57.9	20.04	61.72
		Coontail	4.8	1.66	
	2.	Eelgrass	120.8	11.24	
		Eelgrass	165.1	15.36	
		Eelgrass	28.3	2.63	
	3.	Eurasian milfoil	38.3	3.52	
		Eurasian milfoil	30.3	2.79	
		Eurasian milfoil	5	0.46	
	4.	Slender naiad	0.8	0.10	
	5.	Water stargrass	42	3.82	
		Water stargrass	1.1	0.10	
Eagle Point	1.	Coontail	24.4	8.45	70.96
		Coontail	103.5	35.83	
	2.	Eelgrass	46.6	4.33	
		Eelgrass	72.8	6.77	
		Eelgrass	1	0.09	
	3.	Eurasian milfoil	96	8.83	
	4.	Water stargrass	19.5	1.77	
		Water stargrass	53.7	4.88	

Appendix IV. Results of September North Basin Survey. Data are reported as blotted dry weight and dry weight converted. The latter is calculated from blotted dry weight/ oven dried weight ratios*.

Site	Species #	Species	Blotted Wet Weight (g)	Final DW (g)	Total DW Per site (g)
Pebble Beach	1.	Coontail	37.1	12.84	97.32
		Coontail	125.9	43.58	
		Coontail	2.9	1.00	
		Coontail	98.23	7.21	
	2.	Ditch grass	50.4	9.45	
	3.	Eelgrass	11.6	1.08	
	4.	Eurasian milfoil	162.5	14.94	
Sand Pt. North	1.	Coontail	13.5	4.67	33.23
	2.	Eelgrass	74.3	6.91	
		Eelgrass	29.2	2.72	
	3.	Eurasian milfoil	47.1	4.33	
		Eurasian milfoil	158.8	14.60	
Wilkins Creek	1.	Coontail	14.3	4.95	61.12
		Coontail	4.5	1.56	
	2.	Eelgrass	150.8	14.03	
		Eelgrass	58.3	5.42	
		Eelgrass	229.2	21.32	
	3.	Eurasian milfoil	85.9	7.90	
		Eurasian milfoil	14.5	1.33	
	4.	Water stargrass	50.7	4.61	